

Gene expression in mouse thyrotrope adenoma: transcription elongation factor stimulates proliferation

Peter Gergics¹, Helen C. Christian², Monica S. Choo¹, Adnan Ajmal^{1,3}, Sally A. Camper¹

¹ Department of Human Genetics, University of Michigan, 1301 Catherine St, Ann Arbor, MI-48109, USA

² Department of Physiology, Anatomy and Genetics, South Parks Rd, University of Oxford, Oxford OX3 0RZ

³ Department of Internal Medicine, Metabolism, Endocrinology and Diabetes, University of Michigan, 1000 Wall Street, Ann Arbor, MI-48105, USA

Abbreviated Title: Transcriptional regulation of thyrotrope hyperplasia

Keywords: pituitary hyperplasia, thyrotrope, transcription factor, endoplasmic reticulum stress, unfolded protein response

Word count: 5,931

Number of figures and tables: 7

Corresponding author and person to who reprint requests should be addressed:

Sally A. Camper PhD

Margery H. Shaw Distinguished University Professor, Professor of Human Genetics

Department of Human Genetics

University of Michigan

5704 Medical Science II Bldg., 1241 E. Catherine St., Ann Arbor, MI 48109-5618

Phone: +1-734-763-0682

Fax: +1-734-763-5831

E-mail: scamper@umich.edu

Disclosure statement: The authors have nothing to disclose.

Abstract

Thyrotrope hyperplasia and hypertrophy are common responses to primary hypothyroidism. To understand the genetic regulation of these processes, we studied gene expression changes in the pituitaries of *Cga*^{-/-} mice, which are deficient in the common alpha subunit of TSH, LH and FSH. These mice have thyrotrope hypertrophy and hyperplasia and develop thyrotrope adenoma. We report that cell proliferation is increased, but the expression of most stem cell markers is unchanged. The alpha subunit is required for secretion of the glycoprotein hormone beta subunits, and mutants exhibit elevated expression of many genes involved in the unfolded protein response, consistent with dilation and stress of the endoplasmic reticulum. Mutants have elevated expression of transcription factors that are important in thyrotrope function, such as *Gata2* and *Isl1*, and those that stimulate proliferation, including *Nupr1*, *E2f1* and *Etv5*. We characterized the expression and function of a novel, over-expressed gene, transcription elongation factor A (SII)-like 5 (*Tceal5*). Stable expression of *Tceal5* in a pituitary progenitor cell line is sufficient to increase cell proliferation. Thus, *Tceal5* may act as a proto-oncogene. This study provides a rich resource for comparing pituitary transcriptomes and an analysis of gene expression networks.

Introduction

Thyrotropes make up to 5-10 % of all cells in the adult pituitary gland. These cells are essential for thyroid development and function, growth, and homeostasis, but our knowledge of how they arise from undifferentiated progenitors is incomplete. *Pou1f1* is expressed at E13.5 in the mouse pituitary gland and is required for development of somatotropes, lactotropes and thyrotropes (1-4). The signature markers of a thyrotrope are choriogonadotropin-alpha (*Cga*) and **TSH-beta** (*Tshb*). *Cga* is expressed first in the rostral tip at embryonic day 11.5 (E11.5) and later in the caudo-medial AL cells, while *Tshb* expression is detected in both areas at E14.5 (5). *Tshb* expression in the caudo-medial area is *Pou1f1* dependent, but POU1F1-negative, TSHB-positive cells exist in neonatal mice (6,7). The gonadotropes express *Cga* and **LH-beta** (*Lhb*) or **FSH-beta** (*Fshb*) from E15.5 and E16.5 respectively, and the mature gonadotropes may emerge from TSH, FSH double positive cells (5,8).

The factors that drive *Pou1f1* progenitors towards a thyrotrope fate are not known. *Gata2* is expressed in gonadotropes and thyrotropes, and it acts synergistically with POU1F1 to stimulate *Tshb* expression (9,10). However, *Gata2* is not essential for thyrotrope or gonadotrope differentiation (11). Mice with a pituitary specific knock out of *Gata2* have fewer gonadotropes and thyrotropes at birth, and the function of these cells is modestly impaired. Several other factors have been implicated in *Tshb* expression, including LHX3, PITX1/2, NR4A1, TRAP220, NCOR, EYA3, SIX1, TEF and HLF, but none have been shown to be exclusively necessary for the thyrotrope fate (10,12-15). The Lin11/Isl-1/Mec-3 (LIM)-type homeodomain transcription factor, ISL1, is expressed in gonadotropes and thyrotropes and is necessary for early pituitary development and maximal thyrotrope response to hypothyroidism (7,16,17). It is dispensable for thyrotrope and gonadotrope fate, however (7).

Cga transcription is regulated differently in thyrotropes and gonadotropes. In these **two** cell types overlapping areas of the promoter region have been implicated for cell specific expression. In thyrotropes

Cga expression is regulated by GATA2, PITX1, LHX2/3, MSX1, and ETS or SP1 (14,18-23), but none of these factors are exclusively necessary for thyrotrope fate. In gonadotropes, SF1 (NR5A1), GATA2 and PITX1 are involved in *Cga* expression (reviewed in (22)). In summary, studies of the regulation of *Cga* expression have not uncovered thyrotrope critical factors.

Multiple genetic defects can cause congenital central hypothyroidism, and several pituitary cell lineages can be affected, especially somatotropes and lactotropes together with thyrotropes (24). The somatotropes and lactotropes appear to require thyroid hormone for complete differentiation and/or population expansion. Consistent with this idea, several hypothyroid mouse models exhibit reductions in somatotropes and lactotropes, including the *Tshr^{hyt/hyt}*, *Tpst2^{grt/grt}*, and *Cga^{-/-}* mice (25-29). *Cga^{-/-}* mice have severe hypothyroidism, hypogonadism, infertility, and develop thyrotrope adenomas by 9 mo - 1 year with high penetrance (29). Serum thyroid hormone (TH) is undetectably low, and there is a profound thyrotrope hypertrophy and hyperplasia by 8 wks. The population sizes of cells in the *Pou1f1* lineage are shifted dramatically. Normally the adult pituitary is composed of ~ 40% somatotropes, 30-40% lactotropes, 10% corticotropes, 7-10% gonadotropes, and 5% thyrotropes (30). *Cga^{-/-}* pituitaries have approximately 45-50% thyrotropes, 12.5% somatotropes, only 3% lactotropes, 10% corticotropes and 7% gonadotropes (29,31,32). This and other features are reversible by TH replacement (32). The profound thyrotrope hypertrophy and hyperplasia in *Cga* mutants make them a great tool to study thyrotrope cell specification, proliferation, and response to hypothyroidism.

Materials and Methods

Experimental animals, sample collection, RNA and cDNA preparation

The animal care and use protocol was approved by the University Committee on Use and Care of Animals at the University of Michigan. *Cga^{tm1Sac}* mice were from our stock (29). For gene expression studies pituitaries were collected from 8 wk old mice of each sex and genotype (see specific numbers at each experiment). For absolute quantification studies, pituitaries were collected from 6 wild type and 5-6 null mice at birth (P0), and 4 wks. RNA extraction and cDNA preparation was described previously (33).

Gene expression microarray

RNA was prepared from 24 pituitary samples: 6 males and 6 females per genotype (33). The Illumina TotalPrep RNA Amplification kit was used to prepare biotin-labelled cRNA from 500 ng RNA. 1500 ng cRNA was hybridized to Illumina MouseWG-6 v2.0 Expression BeadChip for 18 hours at 58 C (<http://www.ncbi.nlm.nih.gov/geo/query/acc.cgi?acc=GPL6887>). BeadChips were scanned and signal intensity was recorded with an Illumina iScan. Image data was analyzed and quantile-normalized with Illumina Genome Studio (v2011.1, Data Analysis Software package with Gene Expression Module v1.9.0 and manifest MouseWG-6_V2_0_R2_11278593_A). Probes with a detection p-value equal or less than 0.01 were filtered and genes with a concordance of one were included in the analysis. Our data is available in NCBI-GEO (<http://www.ncbi.nlm.nih.gov/geo/query/acc.cgi?acc=GSE79451>). Genes expressed with a fold change of ≥ 1.5 or ≤ -1.5 in the wild type vs. *Cga*^{-/-} were analyzed with Ingenuity Pathway Analysis software (IPA) (Qiagen).

Quantitative PCR

We confirmed gene expression changes with quantitative PCR using either TaqMan or SYBR Green I assays. SYBR Green primers were designed with Primer BLAST (<http://www.ncbi.nlm.nih.gov/tools/primer-blast/> National Center for Biotechnology Information)

according to the MIQE guidelines (34). Products were confirmed with bidirectional Sanger sequencing. Reactions were performed in triplicate either in the ABI Real-Time PCR 7900HT or 7500 on a 384-well or 96-well platform with all default run parameters and standard reagents. Data was processed using MS Excel 2010, GraphPad Prism 6.01 and REST (35). Results were listed as fold change \pm SEM in the *Cga*^{-/-}. For relative quantification, we used 3 male and 3 female 8 wk old pituitaries for each genotype. Reactions were performed with 50 ng cDNA. For absolute quantification of *Tceal5* transcripts, pituitaries of six wild type and five to six null mice from the ages of birth (P0), 4 weeks, and 8 weeks were collected. A fragment of *Tceal5* cDNA was PCR amplified and gel purified (Qiagen), quantified (Nanodrop) and strand number was defined using http://molbiol.edu.ru/eng/scripts/01_07.html. A calibration curve with ten-fold increments was constructed with *Tceal5* strand numbers of 1E9 to 1E1. Primers and TaqMan assays are provided in the Supplemental Materials and Methods.

Cloning of Tceal5 in situ hybridization probe, Tceal5-EGFP transgene

We amplified a 336 bp piece of the *Tceal5* cDNA (ENSMUST00000066819; primers: 5-TCTCTTCCAGGTACCAGCTACCAGC-3' & 5-TCTAGCTTGCCCTGGCGTGC-3') from a 8-wk-old *Cga*^{-/-} pituitary cDNA and TA-cloned it into the pGEM-T-Easy vector (Promega). The 779 bp *Tceal5* cDNA was cloned together with an in-frame 3' EGFP into the pcDNA3.1(-) vector (Invitrogen). Briefly, the first 779 bp of the *Tceal5* cDNA before the stop and the cDNA of the EGFP (pEGFP, Clontech) were PCR amplified with primers containing extra restriction endonuclease (RE) ends. In the final construct the pieces were ligated through a *KasI* site and inserted between the *XbaI* and *AflIII* sites of pcDNA3.1(-) to produce TCEAL5-EGFP. Using a similar strategy, the EGFP sequence alone was inserted between the *XbaI*/*AflIII* sites in pcDNA3.1(-) to produce EGFP. All plasmids were confirmed by Sanger sequencing.

Tissue processing, in situ hybridization (ISH) and immunohistochemistry (IHC)

Tissues were fixed for 30 min in 4% paraformaldehyde and processed as described previously (7). For generating *Tceal5* probes, plasmid template was cleaved using *SpeI* for sense and *SacII* for antisense, and the antisense template was blunted. Dioxigenin-labelled probes were synthesized as published and purified with Chroma Spin DEPC-H₂O 100 columns (Clontech) (17,36). ISH was performed at 54 C and standard alkaline phosphatase detection (17,36) was modified based on (37): alkaline phosphate was neutralized after 48 hours, slides were counterstained with methyl green (Vector Labs), dehydrated with series of graded ethanols (25-50-70-100%, 1 minutes each) and mounted using Vectamount (Vector Labs). For IHC, we used antibodies listed in Table 1 and further details are described in the Supplemental Materials and Methods. For sequential ISH followed by IHC the IHC staining was developed using the Vectastain Elite ABC kit (Vector Biolabs) with 3,3'-diaminobenzidine substrate.

Cell culture, generation of heterologous cell lines with a stable transgene

The Pit1-triple cell line was a kind gift from Stephen Liebhaber and Nancy Cooke (University of Pennsylvania) and cells were maintained under their published conditions (38). 2E6 Pit1-triple cells were transfected after 24 hours of plating with 4.2 µg of EGFP-pcDNA3.1 or TCEAL5-EGFP-pcDNA3.1 with FuGene6 (3:1 for FuGene6:DNA ratio, Promega). After 72 hours of transfection, cells were selected with 1250 µg/ml G418 for 7 days (Roche). EGFP positive cells were collected with a Sony Biotechnology Synergy iCyt flow cytometer and cultured.

Proliferation and programmed cell death assessment with cultured cells

2E5 TCEAL5-EGFP or EGFP cells were plated in 100 mm dishes. Cells were counted in 0.4% trypan blue from three dishes per transgene type after 4 and 8 days using a Luna automated cell counter (Firmware 2.5.2; default declustering; Logos Biosystems). Three aliquots were measured from each

plate. Nine data points per group were compared with Mann-Whitney U-test, with significance level set to 0.05. 1E5 TCEAL5-EGFP or EGFP cells per well were plated in 12-well cluster plates. 24 hours later apoptosis was detected using the TMR red In Situ Cell Death Detection Kit (Roche) in 9 wells along with additional wells for positive and negative controls. Nuclei were stained with 4',6-diamidino-2-phenylindole (DAPI). Cells were imaged on the TMR red and DAPI channels with a Leica DMIRB inverted microscope. DAPI+ nuclei were counted automatically and terminal deoxynucleotidyl transferase dUTP nick end labeling (TUNEL+, TMR red+) cells were manually counted with ImageJ. A third of the DAPI images were manually counted as well. The percentage of TUNEL+/DAPI+ cells was compared with SPSS v22 (IBM). These values were tested for normal distribution and homogeneity with Shapiro-Wilk and Levene test, and the means were compared with one-way ANOVA and Scheffe post-hoc test.

Live cell imaging

Cells in culture were imaged using the Olympus FluoView 500 inverted confocal microscope with argon laser (488 nm) and overlaid with bright field images. Dishes were kept in a Pathology Devices LiveCell stage top incubator controlled for 5% CO₂ and 37 C. Individual cells at high resolution were imaged using a chambered cover glass (Nunc Lab-Tek). For videos, the images for the z-stack were compiled using 0.5 µm numerical aperture, 100x oil immersion objective, 2x digital zoom, at 1024x1024 pixel resolution.

Proliferation assessment with 5-ethynyl-2'-deoxyuridine incorporation

Eight week old mice (3 wild types and 3 nulls) were administered 50 µg/g body weight 5-ethynyl-2'-deoxyuridine (EdU) dissolved in dimethyl sulfoxide through intraperitoneal injection. Mice were sacrificed after 2 hours. EdU staining was done on coronal sections from the midrange of the slide series

that contained all pituitary lobes. The Click-iT EdU Imaging kit with Alexa Fluor 488 dye (Thermo Fisher Life Technologies) was utilized as described in Supplemental Materials and Methods. When combined with ISH the ISH was performed first. Slides were imaged as described before (17). ImageJ was used for manually counting DAPI and EdU positive cells. EdU/DAPI ratios were compared with SPSS as described above.

Electron microscopy studies

For electron microscopy analysis, pituitary glands were processed and analyzed as described previously (39). Briefly, the tissue was contrasted with uranyl acetate (2% (w/v) in distilled water) at room temperature, dehydrated in methanol and embedded in LR Gold resin at -20C. Ultrathin sections (50-80 nm) were prepared using a Reichart-Jung ultracut microtome and mounted on nickel grids (Agar Scientific, UK). Sections were immunolabelled for TSH for 2h at room temperature with rabbit anti-mouse TSH primary antibody followed by a 1h incubation with a 15nm gold-conjugated goat anti-rabbit secondary antibody (British Biocell). Antibodies are further described in Table 1. All antibodies were diluted in 0.1M PBS (containing 0.1% egg albumin). Specificity of antibody labelling was confirmed by the absence of labelling in negative control sections in which the primary antibody was replaced with non-immune serum. Finally, sections were counterstained with lead citrate and uranyl acetate and examined on a JOEL 1010 transmission electron microscope (JOEL, USA).

Results

Thyrotropes in *Cga*^{-/-} mice have dilated endoplasmic reticulum filled with TSH beta subunit

Thyrotrope hypertrophy is evident in 3 week and 8 week old *Cga*^{-/-} mice, but not at birth, and increased *Tshb* mRNA has been documented in 8 week old mutants by **ISH** and Northern blotting (29,32). To quantify the progressive increase in *Tshb* expression during development, we carried out qPCR analysis of pituitaries from mutants and wild types at birth, 4 weeks and 8 weeks. Fold changes in *Tshb* transcripts were 2.7 ± 0.5 at birth, 12.0 ± 2.3 at 4 weeks and 89.9 ± 15.2 at 8 weeks ($p=0.001$ for all) (Figure 1A). Thyrotrope hypertrophy in *Cga* mutants is similar to that observed in radio-thyroidectomized mice, but the thyrotrope hyperplasia is more extensive (29). To compare the cellular effects of hypertrophy in *Cga* mutants to that reported for other hypothyroid models, we examined the ultrastructure of thyrotropes in 8 week old *Cga*^{-/-} by transmission electron microscopy. Thyrotropes have about two times the diameter of the wild type ones (Figure. 1B top). The cisternae of the endoplasmic reticulum (ER) are normally thin and elongated and comprise only a small portion of the cytoplasm. The mutant ER appears quite different. Virtually the entire cytoplasm of the cell is filled with dilated ER cisternae (Figure 1B bottom). Dilated ER is consistently found in the majority of mutant thyrotropes, but about one in ten thyrotropes had a mix of smaller and larger cisternae. There are very few secretory granules in the mutant thyrotropes, probably because heterodimerization of CGA and TSHB is required for TSH secretion (40). The mutant mitochondria are more electron dense than in controls, and are in close contact with the ER. The mutant cristae are markedly electron dense and separated by electro lucent sheets. This mitochondrial phenotype is similar to that reported following exposure to oxidative stress (41,42). These findings suggest disrupted thyrotrope function in the cellular compartments responsible for energy production and protein synthesis, folding, assembly and secretion.

Increased proliferation in *Cga*^{-/-} pituitaries

Cga mutants exhibit progressive pituitary hyperplasia, and one year old mutants have pituitaries that are ~5-50x normal size with transplantable adenomatous tumors that retain thyroid hormone responsiveness (43). To assess the proliferation rate at 8 weeks, we injected mice with EdU to mark cells in DNA synthesis or S phase. A small fraction of the anterior pituitary cells were labeled in both genotypes (Figure 2A), but it was increased 3.6 fold in *Cga*^{-/-} (100 ± 24 vs. 359 ± 63 , $p=0.002$) (Figure 2C). No co-labeling with TSH antibodies and EdU was observed in either genotype (Figure 2B). The thyrotrope population is comprised of POU1F1 positive and negative cells (Figure 2D). This suggests that the thyrotropes are quiescent at this age and that there may be multiple routes to develop new thyrotropes.

Expected expression changes in cell lineage specific genes in *Cga*^{-/-} pituitaries

The increase in thyrotropes at the expense of somatotropes and lactotropes provides a unique opportunity to identify genes that drive thyrotrope fate and play roles in thyrotrope hypertrophy and hyperplasia. We performed a microarray experiment to identify differentially expressed genes in the *Cga*^{-/-} pituitary. To assess the success of the experimental design, we examined changes in the expression of signature genes for the main differentiated pituitary cell lineages. As expected, the thyrotrope-related genes *Trhr*, *Gata2* and *Isl1* were up regulated, and *Cga* was down regulated (Table 2A). Transcription factors related to the somatotropes and lactotropes were down regulated, including *Stat5a*, *Smad3* and *Pou1f1*. There is no gross change in the gonadotrope cell number (31,32), and the gonadotrope transcription factors *Nr5a1* and *Egr1* (44) were unchanged. *Gnrhr* was down regulated as expected for hypogonadal mice (45). *Tbx19*, a marker for corticotropes, was unchanged.

Elevated expression of genes involved in immune response, ER stress, unfolded protein response, protein degradation, and transcription

Microarray analysis revealed 846 differentially expressed genes with a fold change of 1.5 or greater (Table 2B). IPA and Database for Annotation, Visualization and Integrated Discovery (DAVID) software were limited for pathway analysis because a quarter of the differentially expressed genes were not annotated. To overcome this we performed extensive literature analysis of genes using BioGPS (www.biogps.org), NCBI PubMed Gene RIFs (Reference Into Functions, <http://www.ncbi.nlm.nih.gov/gene>) and Mouse Genome Informatics (<http://www.informatics.jax.org/>). The main gene clusters are summarized in Table 2C (See also Supplemental Tables 1, 2). The adenoma might be responsible for the 42 immune response related genes (46). Clusters of genes related to ER stress, unfolded protein response, and protein degradation were mostly up regulated, possibly due to the requirement for breaking down the TSH beta subunit (Table 3A). In addition, there were subclusters of genes in connection with mRNA processing (21 total), amino acid metabolism (13 total), post-translational modifications (102 total), vesicular transport (22 total) and exocytosis (14 total). We found 17 genes with proteins located in the ER and the Golgi that were associated with posttranslational modification (glycosylation: 5 up: *Ddost*, *Stt3b*, *Colgalt2*, *Gnptg*, *Galnt18*, 6 down: *Gyltl1b*, *B3gnt8*, *Galnt10/11/16*, *Csgalnact1*; sialization (*St3gal1/6*); sulphatation (*Hs6st1/2*, *Chst8/10*)). The growth factor signaling group of genes (30 total) included TGFB (5 total), the Wnt pathway (13 total), the small GTP-ases (24 total), and the phospholipase C / protein kinase C (13 total) as second messengers. To understand the mechanism of increased cell proliferation, we explored the 60 differentially expressed transcription factor complex genes.

Tceal5 is a novel regulator of cell proliferation

Using qPCR we validated differential expression of 80.5% of the genes with the highest expression levels (33/41, Table 3A). Among these genes were 6 Zn-finger transcription factors, 4 basic helix-loop-helix, 3 basic leucine-zipper, 3 LIM-homeodomain and 6 in various other transcription factor families. In

addition, there were 11 genes that participate in the transcription machinery and elongation. The most up regulated transcription factor gene was *Nupr1* (aka p8, 46.9 ± 12.4 fold; $p=0.001$), which is not essential for thyrotrope specification but important for cell proliferation and involved in adenoma formation (47-50). Two other highly expressed genes, *Etv5* and *E2f1* (3.1 ± 0.8 and 3.6 ± 0.9 fold, respectively, $p=0.001$), have known roles in pituitary cell proliferation, (51,52). We undertook investigation of the second most highly elevated gene, *Tceal5*, (4.1 ± 1.5 fold, $p=0.001$) because its function is unknown. Although *Tceal5* transcripts increase with age in pituitaries of both normal and mutant animals at birth, 4 and 8 weeks, the levels were consistently elevated in the mutants ($p \leq 0.011$ in all pairs, Figure 3A). We examined the expression of other TCEAL family genes and found that *Tceal3* was unchanged (1.0 ± 0.2 fold, $p=0.323$) while *Tceal6* was slightly decreased (-2.2 ± 0.5 fold, $p=0.001$).

Tceal5 is expressed in the anterior and intermediate lobes of the adult pituitary

Robust *Tceal5* expression is limited to the adult pituitary, brain, and pancreatic beta cells (NCBI GEO / BioGPS (<http://ds.biogps.org/?dataset=GSE10246&gene=331532>)). We used ISH to assess regional specific expression in the pituitary gland, and found scattered distribution of positive cells in the anterior and intermediate lobes but not in the posterior lobe (Figure 3B). The distribution of labeled cells is similar in the intermediate lobes of wild type and *Cga* mutant mice. The ALs of wild type mice had intensely stained cells in the wedge area, and the *Cga*-nulls had positive cells in the area adjacent to the wedge. These regions are enriched in pituitary progenitors (53). *Tceal5* expression did not coincide with TSHB in the wild types (Figure 3C). In the mutants a small portion of *Tceal5* positive cells was TSHB positive and many *Tceal5* expressing cells were located near thyrotrope clusters (Figure 3C). About a quarter of the proliferating (EdU+) cells were *Tceal5* positive in both genotypes (25% vs 28.6% in the mutant) (Figure 3D).

We examined the expression of stem cell markers because *Tceal5* was expressed in a region of the pituitary that is enriched for progenitors. SOX2 immunostaining was indistinguishable in mutant and wild type pituitaries, and there was no overlap with EdU staining at 8 wks (data not shown). The microarray did not detect any elevation in expression of stem cell markers. To determine whether there were changes in stem cell marker gene expression that were missed by the microarray, we measured the expression of 16 such genes by qPCR: *Ccnd1*, *c-kit*, *Egf*, *Sox2*, *Sox9*, *Bmi1*, *Nestin*, *Sca1*, *Hesx1*, *Pitx2*, *Sl00b*, *CD133*, *Ki67*, *Gfra2*, *Prop1*, and *Gfap*. Most were unchanged, but there were modest changes in *Ccnd1* and *c-kit* (-1.6 ± 0.4 , $p=0.023$ and 1.6 ± 0.4 , $p=0.009$, respectively). If the stem cell pool is activated to produce new thyrotropes, it is not evident in 8 wk old mice.

Tceal5 increases proliferation of *Pou1f1* expressing progenitors

Tceal5 is not expressed in any of the rodent pituitary cell lines that we analyzed, including the rat somatotrope GH3 cells, mouse pre-gonadotrope α T3-1, mouse corticotrope ATT-20, and Pit1-triple, which expresses POU1F1 and the lineage-specific differentiation markers GH, prolactin (PRL), CGA and TSHB (data not shown) (38). To study the role of *Tceal5* in proliferation, we generated populations of Pit1-triple cells that stably express either a TCEAL5-EGFP fusion protein or EGFP only. Confocal microscopy showed that TCEAL5-EGFP localizes to the nucleus, and EGFP is in the cytoplasm and the secretory vesicles (Figure 3E, and Supplemental Videos 1-3.). Equal numbers of cells were plated, and 4 and 8 days later the number of TCEAL5-EGFP cells were significantly increased relative to cells expressing EGFP alone (Figure 3F; Day 4: $4.4E5 \pm 0.8E5$ vs. $8.7E5 \pm 0.9E5$; Day 8: $37.1E5 \pm 6.1E5$ vs. $58.7E5 \pm 3.7E5$ respectively; $N=9$ at each time point; $p<0.01$). To determine whether TCEAL5 decreased the rate of apoptosis we performed TUNEL assays. 24 hours after plating equal numbers of EGFP and TCEAL5-EGFP cells into cluster plates we found no significant decrease in apoptosis rate (TUNEL+/DAPI+ percentages: $7.30\% \pm 2.36$ vs. $4.48\% \pm 0.88$ in the TCEAL5-EGFP; $N=9$ each; $p=0.07$;

Figure 3G). Thus, *Tceal5* expression is sufficient to enhance proliferation of POU1F1-positive pituitary progenitors.

Protein sequence comparisons among TCEAL family members

We compared the amino acid composition of mouse TCEAL proteins and found that they all share the conserved brain expressed protein domain (BEX, pfam04538, Figure 4A). TCEAL5 is ~80% identical to TCEAL3 and 6 but only ~20-30% identical to TCEAL1, 7, and 8. Mammalian TCEAL5 proteins are highly conserved. Proteins of human, dog, chimpanzee and horse are 82% (164/200) similar (Figure 4B). The BEX3 pro-apoptotic and regulatory functions are defined (Figure 4C), and mouse BEX3 and human TCEAL7 tumor suppressors have similar functions (54-57). We compared mouse TCEAL5 to these two proteins, and although the BEX domain is conserved, TCEAL5 diverges in adjacent regions. Thus, it is not surprising that the proto oncogenic functions of TCEAL5 are different than TCEAL7.

Discussion

Primary hypothyroidism causes thyrotrope hyperplasia and hypertrophy

Primary hypothyroidism stimulates the pituitary to increase TSH production and secretion because of the loss of negative feedback by thyroid hormone (58). Fetal thyrotropes become active late in gestation (59), and the size of the population increases in the postnatal period in response to TRH (60). After birth, low serum thyroid hormone levels affect multiple cell lineages (Supplemental Table 3)(27-29,32,61-63). This characteristically includes an increase in overall thyrotrope cell size, first described as the thyroidectomy

cell population, and a 1.5 to ~10-fold increase in thyrotrope cell number. Interestingly, this is coupled with a substantial decrease in the somatotropes and lactotropes. Because these three specialized cell types are *Pou1f1*-dependent, the expansion of thyrotropes may occur at the expense of the other two cell types (1). In support of this idea, hypothyroid mice and rats exhibit similar changes in cell populations whether the hypothyroidism is generated by ablation of the thyroid gland genetically (64), chemically (62,63) or surgically (61), or via a genetic defect in the TSH synthesis (27,29,31,32) and/or action (28,32)(Supplemental Table 3). We cannot rule out the involvement of different mechanisms, however. To our knowledge, no comprehensive pituitary gene expression analysis has been done previously using any of these models of hypothyroidism. The *Cga*^{-/-} mice have robust thyrotrope hyperplasia, making them a useful model to study gene expression changes associated with expansion of the thyrotrope population. Gene expression changes will also reflect the shift in proportions of other cell types, the reduced or undetectable levels of gonadal steroids and thyroid hormone, respectively, and cellular changes associated with the inability to secrete heterodimeric glycoprotein hormones.

ER distension and subunit coupling defect in *Cga*^{-/-} thyrotropes

Hypothyroidism causes thyrotrope hypertrophy, which is partially reversible by thyroid hormone administration (27,28,31,32,61-64). Ultrastructure analysis has revealed increased cisternae in the endoplasmic reticulum and an increase in secretory granules in various hypothyroid mice (28,61-63,65). We observed similar effects on the ER in *Cga*^{-/-} mice, but we observed very few secretory granules. The paucity of secretory granules is likely due to their inability to secrete TSHB in the absence of the alpha subunit (40,66-69).

The heterodimerization of CGA with TSHB, FSHB, LHB, and chorionic gonadotropin (CGB) occurs in the ER, and beta subunits are required to dimerize with CGA for specific activation of the corresponding receptors (40,66-70). CGA and LHB can be secreted without heterodimerization, but they are

differentially glycosylated (40,71). Thus, the mutant gonadotropes are normal-sized while being capable of secreting the LHB monomer and undergoing hypertrophy in response to hypogonadotropic hypogonadism if thyroid hormone is replaced (31,32). In contrast, the *Cga*^{-/-} mouse thyrotrope is stimulated to overproduce the TSH beta subunit but cannot secrete it. Thus, TSH beta needs to be eliminated through alternative mechanisms.

Excess, uncoupled TSHB triggers multiple cellular responses

Protein quality control starts during the synthesis of the nascent protein at the ER bound ribosome (72). Protein complexes of multiple subunits are common. Many familiar examples come from the immune system, such as the T- and B-cell receptors and the main histocompatibility complex (MHC) class I and II molecules (73-75). The inhibin and activin subunit complexes are examples from the endocrine system (76). The machinery used for protein quality control includes ER resident heat shock proteins *Hspa5*, *Hsp90b1*, *Dnajc1*, *Sec63*, *Dnajb9* to *11*) and folding enzymes (peptidyl-prolyl isomerases (PPIs), FK506 (rapamycin)-binding proteins (FKBPs), carbohydrate binding proteins (calnexins, calreticulins), and protein disulfide isomerases (PDIs eg. *ERp57*))(72,73). *Cga*^{-/-} pituitaries have 41 differentially expressed genes in the unfolded protein response/ER stress cluster, including *Pdia4/6/3*, *Hspa5*, *Hsp90b1*, *Dnajb11/9*, *Ppib*, and *Fkbp14/11/2* (Table 3A). Among these, *Hspa5* is considered to be the master regulator of the downstream ER stress response (72,73,77). We found 17 up regulated genes related to immune functions, including MHC II antigen presentation, and 17 differentially expressed genes associated with glycosylation, sialization, and sulphation in the ER and Golgi. Transfer of various glycosides, sulfate and sialo groups to CGA and TSHB are indispensable for heterodimerization (71,78-84) and receptor activation (66,80,85,86). We hypothesize that some of the same pathways involved in processing TSH subunits are involved in regulating dimerization of other complex proteins. Alternatively, increased expression of immune system genes could be related to responsiveness to tumor

development or eliminating stressed pituitary cells. Pituitary folliculostellate cells have phagocytosis functions that remove degenerating cells (87-89), and they present consumed antigens via the MHC II pathway (90).

ER stress response involves proteasomal and lysosomal degradation

There are at least three known unfolded protein response regulatory pathways distinguished by the ER sensor protein, such as IRE1A (inositol-requiring transmembrane kinase/endonuclease A), PERK (protein kinase R-like endoplasmic reticulum kinase) and ATF6 (activating transcription factor 6) which mediate signaling from the stressed ER to the nucleus (91). The response involves transcriptional regulation of genes in ER protein quality control, ubiquitin-mediated proteasomal degradation complex (ERAD: ER-associated degradation), antioxidant response, amino acid metabolism, lipid and membrane lipid biogenesis, and the secretory machinery (92). In *Cga*^{-/-} pituitaries, the most active pathways involve PERK and ATF6. Downstream target genes for PERK include *Ddit3*, which we confirmed to be differentially expressed (2.2±0.5 fold, p= 0.001). *Creb3l1* is highly similar to *Atf6* and our data confirmed a significant increase in its expression (3.7±1.0 fold, p=0.001) (93). We found many up regulated genes for proteasomal degradation, vesicular transport, and an array of amino acid and lipid metabolism genes. Many genes involved in vesicular transport have roles in ER to Golgi transportation (i.e. *Copg2*, *Tmed2/3/9*, *Sec11*). The quantity of genes associated with lysosomal protein degradation clearly implicates this as an operative mechanism. These results are consistent with an active ER stress response along with upregulated downstream targets, protein degradation, and amplified vesicular transport function.

Chronic ER stress can trigger apoptosis via the mitochondrial pathway (BCL-2 protein family members) and by long term DDIT3 expression (91,94). *Cga*^{-/-} mice have decreased expression of pro-apoptotic proteins such as *Bag2/3*, *Bik* and *Gadd45a/g*. We found very little evidence of apoptosis with activated

caspase-3 immunostaining at 8 weeks of age (data not shown). This is consistent with down-regulated *Bag2/3* and *Bik* expression and increased BCL2 expression in the thyrotropes of *Cga*^{-/-} mice treated with thyroid hormone (31). *Gadd45a* is a downstream target of P53, and *Gadd45g* expression is lost in nonfunctioning pituitary adenomas, and gonadotrope adenomas (95,96). The chronic ER stress together with low rates of apoptosis suggests that the adult *Cga*^{-/-} mice manage ER stress with these gene expression changes.

Differentially expressed transcription factors associated with thyrotrope hyperplasia and hypertrophy

We detected increased proliferation in TSHB-negative AL cells in the marginal zone, between the AL and IL, where pituitary stem cells reside (53). We did not detect any substantial differences in the expression of stem cell markers by microarray, qPCR or SOX2 immunohistochemistry. This argues against an expansion of pituitary stem cells in adult *Cga*^{-/-} mice, although we cannot rule out an expansion of stem cells in younger animals.

Up regulated transcriptional regulators may drive cell proliferation and thyrotrope fate (“cell number management”), and down regulated genes may reflect a loss of thyroid hormone stimulation (“hypothyroidism genes”) and fewer somatotropes and lactotropes (“lineage specific genes”). *Klf9* and *Hr* are classic thyroid hormone-regulated genes (97,98). *Id1* overexpression silences *Cga* expression in pituitary pre-gonadotrope (α T3-1) and thyrotrope (α TSH) cell lines, therefore the lack of *Cga* transcripts may lead to decreased *Id1* expression (99). *Foxo1* is expressed in somatotropes (100). Signaling via the GHR and PRLR activates *Stat5a*, and these receptors are expressed in endocrine target tissues and somatotropes and lactotropes (101-103). The decrease in *Pou1f1* is likely due to the decrease in the number of somatotropes and lactotropes, as the increase in thyrotropes is less than the net decrease in the other two cell types. *Spop* is a positive regulator in gastric, prostate, colorectal and kidney cancers. The

elevated expression of *Trp53inp1/2* genes induces cell cycle arrest and inhibits autophagy (104-107). We focused our follow up studies on up regulated transcription factor genes.

Among the top up regulated transcription factor genes were *Nupr1*, *Tceal5*, *Creb3l1*, *E2f1*, *Etv5*, *Gata2*, and *Isl1*. The increase in *Gata2* transcripts was expected because of the increase in thyrotropes, and we recently demonstrated the role of *Isl1* in thyrotrope differentiation and function (7,9). The increases in *Nupr1*, *Creb3l1*, *E2f1* and *Etv5* expression were not anticipated, but elevated expression of these genes is consistent with their established roles in cell proliferation. *Nupr1* is implicated in hypertrophy, cell proliferation, and cancer in the pituitary, pancreas and muscle, though it is not essential for thyrotrope fate (48-50,108). *Atf4* is the target of the PERK-mediated unfolded protein response, which is highly active in *Cga* mutants, and ATF4 upregulates *Nupr1* transcription (91,109). *Creb3l1* also ties into the ER stress regulated pathway (ATF6) (77,91,93). Non-functioning lactotrope and somatotrope adenomas have increased *E2f1* expression (52). Increased *E2f1* expression reduces Wnt/beta-catenin signaling, and we found 12 genes related to Wnt signaling that would be associated with reduced activity (*Ctnna1*, *Wisp1*, *Wnt10a*, *Tle2*) and upregulated Wnt-inhibitor (*Dkk3* 2.8±0.7 fold, p=0.001). However, *Ctnnbip1*, a key node between *E2f1* and Wnt signaling, was downregulated (-2.4±0.6 fold, p=0.001) (110), and there was no evidence for alteration in *Ctnnb*, *Axin2*, or *Lef1* (data not shown). High *Etv5* expression in endometrial carcinoma positively regulates *Nupr1* transcription, epithelial to mesenchymal transition, and myometrial invasion (111). In spermatogonial stem cells, *Etv5* regulates miR-21, which is critical for self-renewal (51). Thus, transcription factor genes involved in thyrotrope fate and cell proliferation were highly expressed in *Cga*^{-/-} pituitaries.

Tceal5 (transcription elongation factor A (SII)-like 5) is the least studied of the most up-regulated transcription factor genes. *Tceal* genes share a BEX (Brain expressed) domain. *TCEAL1* is widely expressed in normal tissues, and low expression exists in squamous cell esophageal cancer (112,113). *TCEAL4* is ubiquitously expressed, and expression is decreased in anaplastic thyroid cancer samples and cell lines of the ovary, cervix, lung, and bladder cancer (114). *TCEAL7* is the most well studied family

member. Its expression is regulated by CpG methylation and it exerts tumor suppressor functions by modulating expression of nuclear factor kappa-light-chain-enhancer of activated B cells (NF- κ B) target genes, *C-MYC* and *CCND1*, in ovarian carcinoma (55-57).

Tceal5 orthologs have been described in mammals (<http://www.ncbi.nlm.nih.gov/gene/?term=tceal5>). *Tceal5* is predominantly expressed in the brain and pituitary gland. It is expressed in the wedge area of the pituitary, which is thought to contain progenitors. We demonstrated increasing expression of *Tceal5* in the *Cga*^{-/-} pituitary over time from birth to 8 weeks of age. Stable overexpression of *Tceal5* in a *Pou1f1* expressing pituitary progenitor cell line was sufficient to increase cell proliferation, consistent with the idea that it might act as a proto-oncogene. Because the related TCEAL7 is thought to act as a tumor suppressor (55) we compared its protein sequences with mouse TCEAL5 and found many notable structural dissimilarities.

There are several other mouse models that are deficient in a unique subunit of a complex protein. As these subunits may be as critical as the CGA is for the TSH assembly, we postulate that these mice may also present with protein misfolding, which leads to ER stress in the cells of a tissue where the complex protein would be normally expressed. In the endocrine system, the inhibin alpha subunit deficient mice are especially suggestive of such a mechanism because they exhibit ovarian granulosa cell or Sertoli cell hyperplasia/tumors at the main site of the normal inhibin alpha subunit expression, and have a constant drive for more Inhibin A/B synthesis due to unrestrained FSH production (76). The same concept of improper complex protein assembly has already been leveraged in many non-endocrine disorders as a disease of protein conformation leading to ER stress and tissue specific phenotypes (115).

In our current work, the robust thyrotrope hyperplasia and hypertrophy in *Cga*^{-/-} pituitaries is intriguing. The thyrotropes of hypothyroid mice consistently present dilated ER associated with the increased production of TSH. The *Cga*^{-/-} mice are unable to couple subunits for secretion, which results in ER stress and upregulation of the unfolded protein response. Not much is known about these pathways in

488 pituitary tumor formation (92). We found up-regulation of thyrotrope specific genes (*Isl1*, *Gata2*) and
489 numerous, relatively novel regulators of cell proliferation: *Nupr1*, *Etv5*, *E2f1* and *Tceal5*. *Tceal5* is
490 sufficient to increase the growth rate of pituitary progenitors, suggesting a role as a proto-oncogene.
491 Further studies in pituitary adenomas are warranted to clarify its role in normal proliferation as well as in
492 human pituitary adenomas. *Tceal5* is encoded on the X chromosome, which may make it compelling to
493 find out whether it is randomly or non-randomly inactivated in females with pituitary hyperplasia or
494 adenomas. Thyrotrope adenomas are extremely rare but they mostly follow the histological and
495 ultrastructural phenotype of the *Cga*^{-/-} pituitary (116). Therefore, thyrotrope adenoma patients are the top
496 ranked candidates in which to look for previously undiscovered *CGA* deficiency and clarify the
497 proliferation features of *TCEAL5* in the human.

498 **Acknowledgements**

499 We would like to thank the University of Michigan Core Facilities: DNA Sequencing (Bob Lyons, Susan
500 Dagenais), Microscopy and Imaging and Flow Cytometry. We thank Michelle Brinkmeier, Shannon
501 Davis, and Alisha John for contributions to the early stages of the work. We thank to Simon J. Rhodes at
502 Indiana University–Purdue University Indianapolis for providing the POU1F1 antibody.

503

504 This work was supported by NICHD R01HD34283 awarded to S.A.C. P.G. is a participant of the
505 International Endocrine Scholars Program of The Endocrine Society. A.A. received support from
506 2T32DK007245-39 (NIH).

507

References

1. Camper SA, Saunders TL, Katz RW, Reeves RH. The Pit-1 transcription factor gene is a candidate for the murine Snell dwarf mutation. *Genomics* 1990; 8:586-590
2. Li S, Crenshaw EB, 3rd, Rawson EJ, Simmons DM, Swanson LW, Rosenfeld MG. Dwarf locus mutants lacking three pituitary cell types result from mutations in the POU-domain gene pit-1. *Nature* 1990; 347:528-533
3. Sornson MW, Wu W, Dasen JS, Flynn SE, Norman DJ, O'Connell SM, Gukovsky I, Carriere C, Ryan AK, Miller AP, Zuo L, Gleiberman AS, Andersen B, Beamer WG, Rosenfeld MG. Pituitary lineage determination by the Prophet of Pit-1 homeodomain factor defective in Ames dwarfism. *Nature* 1996; 384:327-333
4. Simmons DM, Voss JW, Ingraham HA, Holloway JM, Broide RS, Rosenfeld MG, Swanson LW. Pituitary cell phenotypes involve cell-specific Pit-1 mRNA translation and synergistic interactions with other classes of transcription factors. *Genes Dev* 1990; 4:695-711
5. Japon MA, Rubinstein M, Low MJ. In situ hybridization analysis of anterior pituitary hormone gene expression during fetal mouse development. *J Histochem Cytochem* 1994; 42:1117-1125
6. Lin SC, Li S, Drolet DW, Rosenfeld MG. Pituitary ontogeny of the Snell dwarf mouse reveals Pit-1-independent and Pit-1-dependent origins of the thyrotrope. *Development* 1994; 120:515-522
7. Castinetti F, Brinkmeier ML, Mortensen AH, Vella KR, Gergics P, Brue T, Hollenberg AN, Gan L, Camper SA. ISL1 is necessary for maximal thyrotrope response to hypothyroidism. *Mol Endocrinol* 2015; 29:1510-1521
8. Wen S, Ai W, Alim Z, Boehm U. Embryonic gonadotropin-releasing hormone signaling is necessary for maturation of the male reproductive axis. *Proc Natl Acad Sci U S A* 2010; 107:16372-16377

- 531 **9.** Dasen JS, O'Connell SM, Flynn SE, Treier M, Gleiberman AS, Szeto DP, Hooshmand F,
532 Aggarwal AK, Rosenfeld MG. Reciprocal interactions of Pit1 and GATA2 mediate signaling
533 gradient-induced determination of pituitary cell types. *Cell* 1999; 97:587-598
- 534 **10.** Gordon DF, Lewis SR, Haugen BR, James RA, McDermott MT, Wood WM, Ridgway EC. Pit-1
535 and GATA-2 interact and functionally cooperate to activate the thyrotropin beta-subunit
536 promoter. *J Biol Chem* 1997; 272:24339-24347
- 537 **11.** Charles MA, Saunders TL, Wood WM, Owens K, Parlow AF, Camper SA, Ridgway EC, Gordon
538 DF. Pituitary-specific Gata2 knockout: effects on gonadotrope and thyrotrope function. *Mol*
539 *Endocrinol* 2006; 20:1366-1377
- 540 **12.** Garcia M, Fernandez A, Moreno JC. Central hypothyroidism in children. *Endocr Dev* 2014;
541 26:79-107
- 542 **13.** Ohba K, Sasaki S, Matsushita A, Iwaki H, Matsunaga H, Suzuki S, Ishizuka K, Misawa H, Oki
543 Y, Nakamura H. GATA2 mediates thyrotropin-releasing hormone-induced transcriptional
544 activation of the thyrotropin beta gene. *PloS One* 2011; 6:e18667
- 545 **14.** Sloop KW, Meier BC, Bridwell JL, Parker GE, Schiller AM, Rhodes SJ. Differential activation of
546 pituitary hormone genes by human Lhx3 isoforms with distinct DNA binding properties. *Mol*
547 *Endocrinol* 1999; 13:2212-2225
- 548 **15.** Masumoto KH, Ukai-Tadenuma M, Kasukawa T, Nagano M, Uno KD, Tsujino K, Horikawa K,
549 Shigeyoshi Y, Ueda HR. Acute induction of Eya3 by late-night light stimulation triggers TSHbeta
550 expression in photoperiodism. *Curr Biol* 2010; 20:2199-2206
- 551 **16.** Pfaff SL, Mendelsohn M, Stewart CL, Edlund T, Jessell TM. Requirement for LIM homeobox
552 gene Isl1 in motor neuron generation reveals a motor neuron-dependent step in interneuron
553 differentiation. *Cell* 1996; 84:309-320
- 554 **17.** Gergics P, Brinkmeier ML, Camper SA. Lhx4 deficiency: increased cyclin-dependent kinase
555 inhibitor expression and pituitary hypoplasia. *Mol Endocrinol* 2015; 29:597-612

- 556 **18.** Hashimoto K, Yamada M, Monden T, Satoh T, Wondisford FE, Mori M. Thyrotropin-releasing
557 hormone (TRH) specific interaction between amino terminus of P-Lim and CREB binding protein
558 (CBP). *Mol Cell Endocrinol* 2005; 229:11-20
- 559 **19.** Sarapura VD, Strouth HL, Wood WM, Gordon DF, Ridgway EC. Activation of the glycoprotein
560 hormone alpha-subunit gene promoter in thyrotropes. *Mol Cell Endocrinol* 1998; 146:77-86
- 561 **20.** Sarapura VD, Strouth HL, Gordon DF, Wood WM, Ridgway EC. Msx1 is present in thyrotropic
562 cells and binds to a consensus site on the glycoprotein hormone alpha-subunit promoter. *Mol*
563 *Endocrinol* 1997; 11:1782-1794
- 564 **21.** Wood WM, Dowding JM, Gordon DF, Ridgway EC. An upstream regulator of the glycoprotein
565 hormone alpha-subunit gene mediates pituitary cell type activation and repression by different
566 mechanisms. *J Biol Chem* 1999; 274:15526-15532
- 567 **22.** Brinkmeier ML, Gordon DF, Dowding JM, Saunders TL, Kendall SK, Sarapura VD, Wood WM,
568 Ridgway EC, Camper SA. Cell-specific expression of the mouse glycoprotein hormone alpha-
569 subunit gene requires multiple interacting DNA elements in transgenic mice and cultured cells.
570 *Mol Endocrinol* 1998; 12:622-633
- 571 **23.** Glenn DJ, Maurer RA. MRG1 binds to the LIM domain of Lhx2 and may function as a
572 coactivator to stimulate glycoprotein hormone alpha-subunit gene expression. *J Biol Chem* 1999;
573 274:36159-36167
- 574 **24.** Schoenmakers N, Alatzoglou KS, Chatterjee VK, Dattani MT. Recent advances in central
575 congenital hypothyroidism. *J Endocrinol* 2015; 227:R51-71
- 576 **25.** Samuels HH, Forman BM, Horowitz ZD, Ye ZS. Regulation of gene expression by thyroid
577 hormone. *J Clin Invest* 1988; 81:957-967
- 578 **26.** Pernasetti F, Caccavelli L, Van de Weerd C, Martial JA, Muller M. Thyroid hormone inhibits the
579 human prolactin gene promoter by interfering with activating protein-1 and estrogen stimulations.
580 *Mol Endocrinol* 1997; 11:986-996

- 581 **27.** Kobayashi K, Yamamoto K, Kikuyama S, Machida T, Kobayashi T. Impaired development of
582 somatotropes, lactotropes and thyrotropes in growth-retarded (grt) mice. *J Toxicol Pathol* 2009;
583 22:187-194
- 584 **28.** Noguchi T, Kudo M, Sugisaki T, Satoh I. An immunocytochemical and electron microscopic
585 study of the hyt mouse anterior pituitary gland. *J Endocrinol* 1986; 109:163-168
- 586 **29.** Kendall SK, Samuelson LC, Saunders TL, Wood RI, Camper SA. Targeted disruption of the
587 pituitary glycoprotein hormone alpha-subunit produces hypogonadal and hypothyroid mice.
588 *Genes Dev* 1995; 9:2007-2019
- 589 **30.** Nunez L, Villalobos C, Senovilla L, Garcia-Sancho J. Multifunctional cells of mouse anterior
590 pituitary reveal a striking sexual dimorphism. *J Physiol* 2003; 549:835-843
- 591 **31.** Kulig E, Camper SA, Kuecker S, Jin L, Lloyd RV. Remodeling of hyperplastic pituitaries in
592 hypothyroid alpha-subunit knockout mice after thyroxine and 17beta-estradiol treatment: role of
593 apoptosis. *Endocr Pathol* 1998; 9:261-274
- 594 **32.** Stahl JH, Kendall SK, Brinkmeier ML, Greco TL, Watkins-Chow DE, Campos-Barros A, Lloyd
595 RV, Camper SA. Thyroid hormone is essential for pituitary somatotropes and lactotropes.
596 *Endocrinology* 1999; 140:1884-1892
- 597 **33.** Mortensen AH, MacDonald JW, Ghosh D, Camper SA. Candidate genes for panhypopituitarism
598 identified by gene expression profiling. *Physiol Genomics* 2011; 43:1105-1116
- 599 **34.** Bustin SA, Benes V, Garson JA, Hellemans J, Huggett J, Kubista M, Mueller R, Nolan T, Pfaffl
600 MW, Shipley GL, Vandesompele J, Wittwer CT. The MIQE guidelines: minimum information
601 for publication of quantitative real-time PCR experiments. *Clin Chem* 2009; 55:611-622
- 602 **35.** Pfaffl MW, Horgan GW, Dempfle L. Relative expression software tool (REST) for group-wise
603 comparison and statistical analysis of relative expression results in real-time PCR. *Nucleic Acids*
604 *Res* 2002; 30:e36

- 605 **36.** Polk RC, Gergics P, Steimle JD, Li H, Moskowitz IP, Camper SA, Reeves RH. The pattern of
606 congenital heart defects arising from reduced Tbx5 expression is altered in a Down syndrome
607 mouse model. *BMC Dev Biol* 2015; 15:30
- 608 **37.** Gaston-Massuet C, Henderson DJ, Greene ND, Copp AJ. Zic4, a zinc-finger transcription factor,
609 is expressed in the developing mouse nervous system. *Dev Dyn* 2005; 233:1110-1115
- 610 **38.** Sizova D, Ho Y, Cooke NE, Liebhaber SA. Research resource: T-antigen transformation of
611 pituitary cells captures three novel cell lines in the Pit-1 lineage. *Mol Endocrinol* 2010; 24:2232-
612 2240
- 613 **39.** Abel MH, Charlton HM, Huhtaniemi I, Pakarinen P, Kumar TR, Christian HC. An investigation
614 into pituitary gonadotrophic hormone synthesis, secretion, subunit gene expression and cell
615 structure in normal and mutant male mice. *J Neuroendocrinol* 2013; 25:863-875
- 616 **40.** Matzuk MM, Kornmeier CM, Whitfield GK, Kourides IA, Boime I. The glycoprotein alpha-
617 subunit is critical for secretion and stability of the human thyrotropin beta-subunit. *Mol*
618 *Endocrinol* 1988; 2:95-100
- 619 **41.** Cole NB, Daniels MP, Levine RL, Kim G. Oxidative stress causes reversible changes in
620 mitochondrial permeability and structure. *Exp Gerontol* 2010; 45:596-602
- 621 **42.** Gronblad M, Akerman KE. Electron-dense endoplasmic reticulum-like profiles closely associated
622 with mitochondria in glomus cells of the carotid body after fixation with oxalate. *Exp Cell Res*
623 1984; 152:161-168
- 624 **43.** Brinkmeier ML, Stahl JH, Gordon DF, Ross BD, Sarapura VD, Dowding JM, Kendall SK, Lloyd
625 RV, Ridgway EC, Camper SA. Thyroid hormone-responsive pituitary hyperplasia independent of
626 somatostatin receptor 2. *Mol Endocrinol* 2001; 15:2129-2136
- 627 **44.** Suh H, Gage PJ, Drouin J, Camper SA. Pitx2 is required at multiple stages of pituitary
628 organogenesis: pituitary primordium formation and cell specification. *Development* 2002;
629 129:329-337

- 630 **45.** Wu S, Chen Y, Fajobi T, DiVall SA, Chang C, Yeh S, Wolfe A. Conditional knockout of the
631 androgen receptor in gonadotropes reveals crucial roles for androgen in gonadotropin synthesis
632 and surge in female mice. *Mol Endocrinol* 2014; 28:1670-1681
- 633 **46.** Woo SR, Corrales L, Gajewski TF. The STING pathway and the T cell-inflamed tumor
634 microenvironment. *Trends Immunol* 2015; 36:250-256
- 635 **47.** Million Passe CM, White CR, King MW, Quirk PL, Iovanna JL, Quirk CC. Loss of the protein
636 NUPR1 (p8) leads to delayed LHB expression, delayed ovarian maturation, and testicular
637 development of a sertoli-cell-only syndrome-like phenotype in mice. *Biol Reprod* 2008; 79:598-
638 607
- 639 **48.** Quirk CC, Seachrist DD, Nilson JH. Embryonic expression of the luteinizing hormone beta gene
640 appears to be coupled to the transient appearance of p8, a high mobility group-related
641 transcription factor. *J Biol Chem* 2003; 278:1680-1685
- 642 **49.** Mohammad HP, Seachrist DD, Quirk CC, Nilson JH. Reexpression of p8 contributes to
643 tumorigenic properties of pituitary cells and appears in a subset of prolactinomas in transgenic
644 mice that hypersecrete luteinizing hormone. *Mol Endocrinol* 2004; 18:2583-2593
- 645 **50.** Chowdhury UR, Samant RS, Fodstad O, Shevde LA. Emerging role of nuclear protein 1
646 (NUPR1) in cancer biology. *Cancer Metastasis Rev* 2009; 28:225-232
- 647 **51.** Niu Z, Goodyear SM, Rao S, Wu X, Tobias JW, Avarbock MR, Brinster RL. MicroRNA-21
648 regulates the self-renewal of mouse spermatogonial stem cells. *Proc Natl Acad Sci U S A* 2011;
649 108:12740-12745
- 650 **52.** Zhou C, Wawrowsky K, Bannykh S, Gutman S, Melmed S. E2F1 induces pituitary tumor
651 transforming gene (PTTG1) expression in human pituitary tumors. *Mol Endocrinol* 2009;
652 23:2000-2012
- 653 **53.** Garcia-Lavandeira M, Diaz-Rodriguez E, Bahar D, Garcia-Rendueles AR, Rodrigues JS, Dieguez
654 C, Alvarez CV. Pituitary cell turnover: from adult stem cell recruitment through differentiation to
655 death. *Neuroendocrinology* 2015; 101:175-192

- 656 **54.** Mukai J, Shoji S, Kimura MT, Okubo S, Sano H, Suvanto P, Li Y, Irie S, Sato TA. Structure-
657 function analysis of NADE: identification of regions that mediate nerve growth factor-induced
658 apoptosis. *J Biol Chem* 2002; 277:13973-13982
- 659 **55.** Chien J, Staub J, Avula R, Zhang H, Liu W, Hartmann LC, Kaufmann SH, Smith DI, Shridhar V.
660 Epigenetic silencing of TCEAL7 (Bex4) in ovarian cancer. *Oncogene* 2005; 24:5089-5100
- 661 **56.** Chien J, Narita K, Rattan R, Giri S, Shridhar R, Staub J, Beleford D, Lai J, Roberts LR, Molina J,
662 Kaufmann SH, Prendergast GC, Shridhar V. A role for candidate tumor-suppressor gene
663 TCEAL7 in the regulation of c-Myc activity, cyclin D1 levels and cellular transformation.
664 *Oncogene* 2008; 27:7223-7234
- 665 **57.** Rattan R, Narita K, Chien J, Maguire JL, Shridhar R, Giri S, Shridhar V. TCEAL7, a putative
666 tumor suppressor gene, negatively regulates NF-kappaB pathway. *Oncogene* 2010; 29:1362-1373
- 667 **58.** Roelfsema F, Pereira AM, Adriaanse R, Endert E, Fliers E, Romijn JA, Veldhuis JD. Thyrotropin
668 secretion in mild and severe primary hypothyroidism is distinguished by amplified burst mass and
669 Basal secretion with increased spikiness and approximate entropy. *J Clin Endocrinol Metab* 2010;
670 95:928-934
- 671 **59.** Beamer WG, Cresswell LA. Defective thyroid ontogenesis in fetal hypothyroid (hyt/hyt) mice.
672 *Anat Rec* 1982; 202:387-393
- 673 **60.** Shibusawa N, Yamada M, Hirato J, Monden T, Satoh T, Mori M. Requirement of thyrotropin-
674 releasing hormone for the postnatal functions of pituitary thyrotrophs: ontogeny study of
675 congenital tertiary hypothyroidism in mice. *Mol Endocrinol* 2000; 14:137-146
- 676 **61.** Surks MI, DeFesi CR. Determination of the cell number of each cell type in the anterior pituitary
677 of euthyroid and hypothyroid rats. *Endocrinology* 1977; 101:946-958
- 678 **62.** Stratmann IE, Ezrin C, Sellers EA, Simon GT. The origin of thyroidectomy cells as revealed by
679 high resolution radioautography. *Endocrinology* 1972; 90:728-734

- 680 **63.** DeFesi CR, Astier HS, Surks MI. Kinetics of thyrotrophs and somatotrophs during development
681 of hypothyroidism and L-triiodothyronine treatment of hypothyroid rats. *Endocrinology* 1979;
682 104:1172-1180
- 683 **64.** Friedrichsen S, Christ S, Heuer H, Schafer MK, Parlow AF, Visser TJ, Bauer K. Expression of
684 pituitary hormones in the Pax8^{-/-} mouse model of congenital hypothyroidism. *Endocrinology*
685 2004; 145:1276-1283
- 686 **65.** Farquhar MG, Rinehart JF. Cytologic alterations in the anterior pituitary gland following
687 thyroidectomy: an electron microscope study. *Endocrinology* 1954; 65:857-876
- 688 **66.** Fares F. The role of O-linked and N-linked oligosaccharides on the structure-function of
689 glycoprotein hormones: development of agonists and antagonists. *Biochim Biophys Acta* 2006;
690 1760:560-567
- 691 **67.** Fares FA, Yamabe S, Ben-Menahem D, Pixley M, Hsueh AJ, Boime I. Conversion of thyrotropin
692 heterodimer to a biologically active single-chain. *Endocrinology* 1998; 139:2459-2464
- 693 **68.** Pierce JG, Parsons TF. Glycoprotein hormones: structure and function. *Annu Rev Biochem* 1981;
694 50:465-495
- 695 **69.** Grossmann M, Wong R, Szkudlinski MW, Weintraub BD. Human thyroid-stimulating hormone
696 (hTSH) subunit gene fusion produces hTSH with increased stability and serum half-life and
697 compensates for mutagenesis-induced defects in subunit association. *J Biol Chem* 1997;
698 272:21312-21316
- 699 **70.** Szkudlinski MW, Thotakura NR, Weintraub BD. Subunit-specific functions of N-linked
700 oligosaccharides in human thyrotropin: role of terminal residues of alpha- and beta-subunit
701 oligosaccharides in metabolic clearance and bioactivity. *Proc Natl Acad Sci U S A* 1995;
702 92:9062-9066
- 703 **71.** Parsons TF, Bloomfield GA, Pierce JG. Purification of an alternate form of the alpha subunit of
704 the glycoprotein hormones from bovine pituitaries and identification of its O-linked
705 oligosaccharide. *J Biol Chem* 1983; 258:240-244

- 706 **72.** Ellgaard L, Helenius A. Quality control in the endoplasmic reticulum. *Nat Rev Mol Cell Biol*
707 2003; 4:181-191
- 708 **73.** Feige MJ, Hendershot LM. Quality control of integral membrane proteins by assembly-dependent
709 membrane integration. *Mol Cell* 2013; 51:297-309
- 710 **74.** van Kasteren SI, Overkleeft H, Ovaa H, Neefjes J. Chemical biology of antigen presentation by
711 MHC molecules. *Curr Opin Immunol* 2014; 26:21-31
- 712 **75.** Vettermann C, Herrmann K, Jack HM. Powered by pairing: the surrogate light chain amplifies
713 immunoglobulin heavy chain signaling and pre-selects the antibody repertoire. *Semin Immunol*
714 2006; 18:44-55
- 715 **76.** Matzuk MM, Finegold MJ, Su JG, Hsueh AJ, Bradley A. Alpha-inhibin is a tumour-suppressor
716 gene with gonadal specificity in mice. *Nature* 1992; 360:313-319
- 717 **77.** Greenwood M, Greenwood MP, Paton JF, Murphy D. Transcription factor CREB3L1 regulates
718 endoplasmic reticulum stress response genes in the osmotically challenged rat hypothalamus.
719 *PloS One* 2015; 10:e0124956
- 720 **78.** Magner JA, Weintraub BD. Thyroid-stimulating hormone subunit processing and combination in
721 microsomal subfractions of mouse pituitary tumor. *J Biol Chem* 1982; 257:6709-6715
- 722 **79.** Magner JA. Thyroid-stimulating hormone: biosynthesis, cell biology, and bioactivity. *Endocr Rev*
723 1990; 11:354-385
- 724 **80.** Grossmann M, Szkudlinski MW, Tropea JE, Bishop LA, Thotakura NR, Schofield PR,
725 Weintraub BD. Expression of human thyrotropin in cell lines with different glycosylation patterns
726 combined with mutagenesis of specific glycosylation sites. Characterization of a novel role for
727 the oligosaccharides in the in vitro and in vivo bioactivity. *J Biol Chem* 1995; 270:29378-29385
- 728 **81.** Weintraub BD, Stannard BS, Linnekin D, Marshall M. Relationship of glycosylation to de novo
729 thyroid-stimulating hormone biosynthesis and secretion by mouse pituitary tumor cells. *J Biol*
730 *Chem* 1980; 255:5715-5723

- 731 **82.** Wopereis S, Lefeber DJ, Morava E, Wevers RA. Mechanisms in protein O-glycan biosynthesis
732 and clinical and molecular aspects of protein O-glycan biosynthesis defects: a review. Clin Chem
733 2006; 52:574-600
- 734 **83.** Grossmann M, Szkudlinski MW, Wong R, Dias JA, Ji TH, Weintraub BD. Substitution of the
735 seat-belt region of the thyroid-stimulating hormone (TSH) beta-subunit with the corresponding
736 regions of choriogonadotropin or follitropin confers luteotropic but not follitropic activity to
737 chimeric TSH. J Biol Chem 1997; 272:15532-15540
- 738 **84.** Fairlie WD, Stanton PG, Hearn MT. Contribution of specific disulphide bonds to two epitopes of
739 thyrotropin beta-subunit associated with receptor recognition. Eur J Biochem 1996; 240:622-627
- 740 **85.** Thotakura NR, LiCalzi L, Weintraub BD. The role of carbohydrate in thyrotropin action assessed
741 by a novel approach using enzymatic deglycosylation. J Biol Chem 1990; 265:11527-11534
- 742 **86.** Weintraub BD, Stannard BS, Meyers L. Glycosylation of thyroid-stimulating hormone in
743 pituitary tumor cells: influence of high mannose oligosaccharide units on subunit aggregation,
744 combination, and intracellular degradation. Endocrinology 1983; 112:1331-1345
- 745 **87.** Harrison F, Van Hoof J, Vakaet L. Processing of cell debris suggestive and phagocytosis in the
746 follicular cavities of the avian adenohypophysis. Cell Biol Int Rep 1982; 6:153-161
- 747 **88.** Orgnero de Gaisan EM, Maldonado CA, Aoki A. Fate of degenerating lactotrophs in rat pituitary
748 gland after interruption of lactation: a histochemical and immunocytochemical study. Histochem
749 J 1993; 25:150-165
- 750 **89.** Claudius L, Yoshimi Y, Yoichiro H, Gabriel M, Koichi M. Phagocytotic removal of apoptotic
751 endocrine cells by folliculostellate cells and its functional implications in clusterin accumulation
752 in pituitary colloids in helmeted guinea fowl (*Numida meleagris*). Acta Histochem 2006; 108:69-
753 80
- 754 **90.** Allaerts W, Vankelecom H. History and perspectives of pituitary folliculo-stellate cell research.
755 Eur J Endocrinol 2005; 153:1-12

- 756 **91.** Hetz C, Martinon F, Rodriguez D, Glimcher LH. The unfolded protein response: integrating
757 stress signals through the stress sensor IRE1alpha. *Physiol Rev* 2011; 91:1219-1243
- 758 **92.** Chaudhari N, Talwar P, Parimisetty A, Lefebvre d'Hellencourt C, Ravanan P. A molecular web:
759 endoplasmic reticulum stress, inflammation, and oxidative stress. *Front Cell Neurosci* 2014;
760 8:213
- 761 **93.** Murakami T, Saito A, Hino S, Kondo S, Kanemoto S, Chihara K, Sekiya H, Tsumagari K, Ochiai
762 K, Yoshinaga K, Saitoh M, Nishimura R, Yoneda T, Kou I, Furuichi T, Ikegawa S, Ikawa M,
763 Okabe M, Wanaka A, Imaizumi K. Signalling mediated by the endoplasmic reticulum stress
764 transducer OASIS is involved in bone formation. *Nat Cell Biol* 2009; 11:1205-1211
- 765 **94.** Iurlaro R, Munoz-Pinedo C. Cell death induced by endoplasmic reticulum stress. *FEBS J* 2015;
- 766 **95.** Michaelis KA, Knox AJ, Xu M, Kiseljak-Vassiliades K, Edwards MG, Geraci M, Kleinschmidt-
767 DeMasters BK, Lillehei KO, Wierman ME. Identification of growth arrest and DNA-damage-
768 inducible gene beta (GADD45beta) as a novel tumor suppressor in pituitary gonadotrope tumors.
769 *Endocrinology* 2011; 152:3603-3613
- 770 **96.** Zhang X, Sun H, Danila DC, Johnson SR, Zhou Y, Swearingen B, Klibanski A. Loss of
771 expression of GADD45 gamma, a growth inhibitory gene, in human pituitary adenomas:
772 implications for tumorigenesis. *J Clin Endocrinol Metab* 2002; 87:1262-1267
- 773 **97.** Dugas JC, Ibrahim A, Barres BA. The T3-induced gene KLF9 regulates oligodendrocyte
774 differentiation and myelin regeneration. *Mol Cell Neurosci* 2012; 50:45-57
- 775 **98.** Thompson CC. Thyroid hormone-responsive genes in developing cerebellum include a novel
776 synaptotagmin and a hairless homolog. *J Neurosci* 1996; 16:7832-7840
- 777 **99.** Jackson SM, Gutierrez-Hartmann A, Hoeffler JP. Upstream stimulatory factor, a basic-helix-
778 loop-helix-zipper protein, regulates the activity of the alpha-glycoprotein hormone subunit gene
779 in pituitary cells. *Mol Endocrinol* 1995; 9:278-291

780 **100.** Majumdar S, Farris CL, Kabat BE, Jung DO, Ellsworth BS. Forkhead Box O1 is present in
781 quiescent pituitary cells during development and is increased in the absence of p27 Kip1. *PLoS*
782 *One* 2012; 7:e52136

783 **101.** Mertani HC, Pechoux C, Garcia-Caballero T, Waters MJ, Morel G. Cellular localization of the
784 growth hormone receptor/binding protein in the human anterior pituitary gland. *J Clin Endocrinol*
785 *Metab* 1995; 80:3361-3367

786 **102.** Morel G, Ouhtit A, Kelly PA. Prolactin receptor immunoreactivity in rat anterior pituitary.
787 *Neuroendocrinology* 1994; 59:78-84

788 **103.** Teglund S, McKay C, Schuetz E, van Deursen JM, Stravopodis D, Wang D, Brown M, Bodner S,
789 Grosveld G, Ihle JN. Stat5a and Stat5b proteins have essential and nonessential, or redundant,
790 roles in cytokine responses. *Cell* 1998; 93:841-850

791 **104.** Kim MS, Je EM, Oh JE, Yoo NJ, Lee SH. Mutational and expressional analyses of SPOP, a
792 candidate tumor suppressor gene, in prostate, gastric and colorectal cancers. *APMIS* 2013;
793 121:626-633

794 **105.** Li G, Ci W, Karmakar S, Chen K, Dhar R, Fan Z, Guo Z, Zhang J, Ke Y, Wang L, Zhuang M, Hu
795 S, Li X, Zhou L, Li X, Calabrese MF, Watson ER, Prasad SM, Rinker-Schaeffer C, Eggen SE,
796 Stricker T, Tian Y, Schulman BA, Liu J, White KP. SPOP Promotes Tumorigenesis by Acting as
797 a Key Regulatory Hub in Kidney Cancer. *Cancer Cell* 2014; 25:455-468

798 **106.** Tomasini R, Seux M, Nowak J, Bontemps C, Carrier A, Dagorn JC, Pebusque MJ, Iovanna JL,
799 Duseti NJ. TP53INP1 is a novel p73 target gene that induces cell cycle arrest and cell death by
800 modulating p73 transcriptional activity. *Oncogene* 2005; 24:8093-8104

801 **107.** Sala D, Ivanova S, Plana N, Ribas V, Duran J, Bach D, Turkseven S, Laville M, Vidal H,
802 Karczewska-Kupczewska M, Kowalska I, Strackowski M, Testar X, Palacin M, Sandri M,
803 Serrano AL, Zorzano A. Autophagy-regulating TP53INP2 mediates muscle wasting and is
804 repressed in diabetes. *J Clin Invest* 2014;

- 805 **108.** Kong DK, Georgescu SP, Cano C, Aronovitz MJ, Iovanna JL, Patten RD, Kyriakis JM, Goruppi
806 S. Deficiency of the transcriptional regulator p8 results in increased autophagy and apoptosis, and
807 causes impaired heart function. *Mol Biol Cell* 2010; 21:1335-1349
- 808 **109.** Passe CM, Cooper G, Quirk CC. The murine p8 gene promoter is activated by activating
809 transcription factor 4 (ATF4) in the gonadotrope-derived LbetaT2 cell line. *Endocrine* 2006;
810 30:81-91
- 811 **110.** Wu Z, Zheng S, Li Z, Tan J, Yu Q. E2F1 suppresses Wnt/beta-catenin activity through
812 transactivation of beta-catenin interacting protein ICAT. *Oncogene* 2011; 30:3979-3984
- 813 **111.** Pedrola N, Devis L, Llauro M, Campoy I, Martinez-Garcia E, Garcia M, Muinelo-Romay L,
814 Alonso-Alconada L, Abal M, Alameda F, Mancebo G, Carreras R, Castellvi J, Cabrera S, Gil-
815 Moreno A, Matias-Guiu X, Iovanna JL, Colas E, Reventos J, Ruiz A. Nidogen 1 and Nuclear
816 Protein 1: novel targets of ETV5 transcription factor involved in endometrial cancer invasion.
817 *Clin Exp Metastasis* 2015; 32:467-478
- 818 **112.** Pillutla RC, Shimamoto A, Furuichi Y, Shatkin AJ. Genomic structure and chromosomal
819 localization of TCEAL1, a human gene encoding the nuclear phosphoprotein p21/SIIR.
820 *Genomics* 1999; 56:217-220
- 821 **113.** Makino H, Tajiri T, Miyashita M, Sasajima K, Anbazhagan R, Johnston J, Gabrielson E.
822 Differential expression of TCEAL1 in esophageal cancers by custom cDNA microarray analysis.
823 *Disea Esoph* 2005; 18:37-40
- 824 **114.** Akaishi J, Onda M, Okamoto J, Miyamoto S, Nagahama M, Ito K, Yoshida A, Shimizu K.
825 Down-regulation of transcription elongation factor A (SII) like 4 (TCEAL4) in anaplastic thyroid
826 cancer. *BMC Cancer* 2006; 6
- 827 **115.** Parmar JS, Lomas DA. Alpha-1-antitrypsin deficiency, the serpinopathies and conformational
828 disease. *J R Coll Physicians Lond* 2000; 34:295-300
- 829 **116.** Alkhani AM, Cusimano M, Kovacs K, Bilbao JM, Horvath E, Singer W. Cytology of pituitary
830 thyrotroph hyperplasia in protracted primary hypothyroidism. *Pituitary* 1999; 1:291-295

Figures and Legends

Figure 1.

***Cga*^{-/-} mice show a progressive increase in *Tshb* mRNA expression from birth to adulthood and present with extremely dilated endoplasmic reticulum (ER) cisternae**

A) Quantitative PCR with relative quantification showing the increase of *Tshb* transcript expression during postnatal life in the *Cga*^{-/-} vs. wild type. B) Transmission electron microscopy showing thyrotropes identified by TSHB antibody staining from a normal and *Cga*^{-/-} mouse pituitary at 8 weeks. Top panels show a low magnification view of the overall difference in the size of a typical thyrotrope shaded with green. Bottom panels depict an area within a typical thyrotrope with the characteristic thin-layered ER structure in wild types and greatly dilated ER in mutants. Also note the decreased number of secretory granules in the mutants, as well as the more electron dense mitochondria. (cap: capillary, nuc: nucleus, g: secretory granule, m: mitochondrion, rer: rough ER)

Figure 2.

Thyrotrope hypertrophy and hyperplasia are associated with proliferation of TSHB-negative cells

A) Pituitaries were stained for EdU, which marks proliferating cells in S-phase with green, and counterstained with DAPI that makes the nuclei blue. B) Pituitary sections stained for TSHB in red, EdU in green and nuclei in blue showed no co-staining of TSHB and EdU in either genotype. Arrows indicate EdU positive cells. Clusters of thyrotropes are interspersed with TSHB negative cells. Scale bar equals to 100 μ m in Panel A/B/D. Mice were at 8 weeks of age. C) The ratio of EdU per DAPI positive cell is increased in the *Cga*^{-/-} mice. Ratio is compared to wild type. D) Thyrotropes stained with TSHB (red) from representative areas of 8 wk old pituitaries show a mix of POU1F1 positive (green) and negative cells in both genotypes. Nuclei were counterstained with DAPI.

Figure 3.

Characterization of TCEAL5 in the pituitary and in a progenitor cell

Panel A. *Tceal5* expression is increased from birth to adulthood in the *Cga*^{-/-} pituitary.

Absolute quantification with qPCR showed an incremental increase in *Tceal5* expression from birth through 4 weeks and 8 weeks of age in 50 ng cDNA; ($p \leq 0.011$ for all pairs).

Panel B. *Tceal5* transcripts are localized in the anterior and intermediate lobes of the pituitary.

Tceal5 is expressed in few AL and IL cells in the wild type and *Cga*^{-/-} pituitaries show an altered distribution. Purple stain marks *Tceal5* while green is nuclear counterstaining. Scale bar equals to 50 μ m in all panels.

Panel C. *Cga*^{-/-} but not wild type pituitaries have *Tceal5* positive thyrotropes

Combined *Tceal5* ISH (purple) with TSHB IHC (brown) and green nuclear counterstaining. In a typical view yellow arrows mark some *Tceal5*⁺/TSHB⁻ and black arrows mark *Tceal5*⁺/TSHB⁺ cells. Note that single *Tceal5*⁺ cells are typically close to thyrotrope clusters.

Panel D. A small portion of proliferating cells express *Tceal5*

Proliferation detected with EdU (green) and *Tceal5* mRNA (purple) over nuclear staining with DAPI (blue). Representative views from both genotypes showing cells with arrows as EdU⁺/*Tceal5*⁺ (black), EdU⁺/*Tceal5*⁻ (yellow) and EdU⁻/*Tceal5*⁺ (red) respectively.

Panel E. Transgenic TCEAL5-EGFP has nuclear expression in the Pit1-triple pituitary progenitor cell line.

Individual cells were imaged with confocal microscopy to determine the localization of EGFP in stable, transgenic cell populations. EGFP without TCEAL5 was localized to the cytoplasm, while the TCEAL5-GFP fusion localized to the nucleus. Scale bar equals 10 μ m.

Panel F. Stable overexpression of *Tceal5* significantly enhances proliferation in a pituitary progenitor cell line.

The Pit1-triple line expresses *Pou1f1*, *Gh*, *Prl*, *Tshb* and *Cga* (38). We created heterologous lines stably expressing a *Tceal5-Egfp* gene fusion or *Egfp*-only and plated the same number of cells on Day 0. Six plates with each were monitored and three each were harvested for cell counting after 4 or 8 days.

Panel G. Stable overexpression of *Tceal5* does not change the apoptosis rate in a pituitary progenitor line

Nine wells in a cluster plate were assayed for apoptosis with the TUNEL assay heterologous cell lines stably expressing *Tceal5-Egfp* gene fusion or *Egfp*-only. Nuclei were counterstained with DAPI and the percentage of TUNEL+ cells were compared. NS: not significant.

Figure 4.

Protein sequence comparison suggests similar and divergent functions for the mouse TCEAL5

Panel A. Conserved domain comparison for mouse TCEAL proteins. (NCBI Conserved Domain search: <http://www.ncbi.nlm.nih.gov/Structure/cdd/cdd.shtml>). TCEAL proteins share the BEX domain and TCEAL3/6 include a ~70 amino acid long segment similar to the conserved DUF2042 domain which has an unknown function.

Panel B. The mouse TCEAL5 protein is highly conserved among mammals.

Q5H9L2, Q8CCT4, E2RDN6, H2R4M4, F6UAE4 protein sequences from the UniProt database (<http://www.uniprot.org/>) for human, mouse, dog, chimpanzee and horse respectively. Symbols mark the following: asterisk - identical, colon/semicolon - similar, hyphen – missing amino acids. The BEX domain is marked with magenta box.

Panel C. Functional domain comparison suggests different functions in proliferation for TCEAL5 compared to related proteins.

Alignment was created with K-Align from the European Bioinformatics Institute (<http://www.ebi.ac.uk/Tools/msa/kalign/>) with default settings and coloring of individual amino acid residues followed the Clustal X color scheme (<http://www.jalview.org/help/html/colourSchemes/clustal.html>). Magenta, translucent blue and green boxes are BEX domain, proapoptotic and regulatory functional domain respectively.

Table 1

Table of antibodies

Table 2

Summary of gene expression changes in the *Cga*^{-/-} pituitary

A) Expression of genes that changed or stayed constant based on expected increased numbers of thyrotropes, decreased numbers of somatotropes and lactotropes, and grossly unchanged numbers of gonadotropes and corticotropes (29,31). All values represent fold changes in the *Cga*^{-/-} pituitaries **B)** Overall numbers of differentially expressed genes with fold change cut-offs of ± 1.5 and ± 2.0 . **C)** Differentially expressed genes were grouped into 18 main categories based on their involvements in

biological processes and molecular functions. The numbers refer to the total number of genes with altered expression in a category, and the subset that are up and down regulated. Some genes can be included in multiple categories. UPR: unfolded protein response, ER: endoplasmic reticulum, GPCR: G-protein coupled receptor, ECM: extracellular matrix

Table 3.

Genes involved in unfolded protein response/endoplasmic reticulum stress and transcription factor complex are elevated in the pituitaries of *Cga*^{-/-} mice

A) Unfolded protein response/ER stress genes are predominantly up regulated and can explain the largely distended ER cisternae that contributes to thyrotrope hyperplasia in *Cga*^{-/-} mice. Table includes gene expression changes from the microarray. B) 33 genes from the transcription factor complex category were confirmed with qPCR in total number of 12 pituitaries (equal number of wild type and mutant mice with equal number of males and females; $p \leq 0.004$).

Supplemental Table 1.

Detailed clusters of genes differentially expressed in the *Cga*^{-/-} pituitary.

Numbers indicate the total genes, up- or downregulated genes in each main and subcategory in *Cga*^{-/-} pituitaries.

Supplemental Table 2.

937 **List of differentially expressed genes in the *Cga*^{-/-} pituitary and their categorization.**

938

939 **Supplemental Table 3.**

940 **Effect of hypothyroidism on pituitary cell population sizes.**

941 These animal models share thyrotrope hyperplasia which is associated with a severe reduction in
942 somatotrope and lactotrope cells and less prominent changes in the gonadotrope and corticotrope lineages.
943 Numbers indicate % of total cells. †: Noguchi et. al in 1986 described striking increase from 10% to
944 77.8% in basophil cells (thyrotropes, gonadotropes and corticotropes together). References are cited in
945 the main text of the paper.

946

947

948 **Supplemental Video 1.**

949 Cell from the native Pit1-triple line. Projected z-stack of confocal images.

950

951 **Supplemental Video 2.**

952 Cell from the Pit1-triple line stably expressing EGFP. EGFP is apparent throughout the whole cell and in
953 the secreting vesicles. Projected z-stack of confocal images.

954

955 **Supplemental Video 3.**

956 Cell from the Pit1-triple line stably expressing mouse TCEAL5-EGFP. EGFP is restricted to the nuclear
957 subcompartment in the cell. Projected z-stack of confocal images.

958

959

960 **Supplemental Materials and Methods**

961 - qPCR primers and TaqMan assays used in the paper.

962 - Protocol for immunohistochemistry with paraffin sections (IHC-P) to detect 5-ethynyl-2'-deoxyuridine
963 (EdU) and rabbit primary antibodies using Tyramide Signal Amplification with sections from formalin-
964 fixed, paraffin embedded tissue.

A

Thyrotrope	Fold change
<i>Cga</i>	-4.55
<i>Trhr</i>	14.58
<i>Gata2</i>	2.53
<i>Isl1</i>	2.55
Gonadotrope	Fold change
<i>Gnrhr</i>	-2.56
<i>Nr5a1</i>	1.10
<i>Egr1</i>	1.18
Somatolactotrope	Fold change
<i>Ghrhr</i>	-2.30
<i>Stat5a</i>	-2.55
<i>Smad3</i>	-1.67
<i>Pou1f1</i>	-3.13
Corticotrope	Fold change
<i>Tbx19</i>	-1.37

B

Fold change cut off	# of genes	Total # of genes
$\geq +1.5$	487	846
≤ -1.5	359	
$\geq +2.0$	157	267
≤ -2.0	110	

C

Main Category	Total	Up	Down
Immune	42	36	6
Protein degradation	35	26	9
UPR/ER stress	41	33	8
Transcription factor	60	30	30
Transport	70	41	29
GPCR	22	11	11
Autophagy	8	2	6
Cell-cell interaction	28	17	11
Endocytosis	23	15	8
Exocytosis	14	9	5
Metabolism	144	80	64
Signaling	190	108	82

Main category	Total	Up	Down
DNA	19	4	15
RNA	42	21	21
ECM	30	16	14
Cytoskeleton	49	28	21
Vesicle	22	12	10

Main category	Total	Up	Down
Unknown	118	61	57

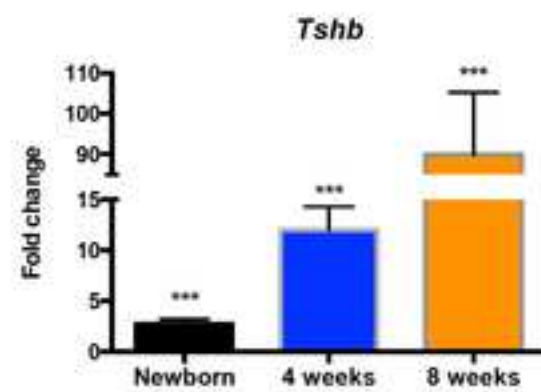
A

Fold change	Entrez Gene ID	Symbol	Gene Name
9.74	76737	<i>Creld2</i>	cysteine-rich with EGF-like domains 2
7.10	64136	<i>Sdf2l1</i>	stromal cell-derived factor 2-like 1
4.64	12304	<i>Pdia4</i>	protein disulfide isomerase family A, member 4
4.18	71853	<i>Pdia6</i>	protein disulfide isomerase family A, member 6
3.25	14828	<i>Hspa5</i>	heat shock 70kDa protein 5 (Grp78)
3.19	22027	<i>Hsp90b1</i>	heat shock protein 90kDa beta (Grp94), member 1
3.07	231440	<i>Parm1</i>	prostate androgen-regulated mucin-like protein 1
2.55	218544	<i>Sgtb</i>	small glutamine-rich tetratricopeptide repeat (TPR)-containing, beta
2.36	231997	<i>Fkbp14</i>	FK506 binding protein 14
2.31	13198	<i>Ddit3</i>	DNA-damage-inducible transcript 3
2.26	67454	<i>Ikbip</i>	inhibitor of nuclear factor kappa-B kinase-interacting protein
2.25	66120	<i>Fkbp11</i>	FK506 binding protein 11
2.24	14227	<i>Fkbp2</i>	FK506 binding protein 2
2.20	66073	<i>Txndc12</i>	thioredoxin domain containing 12 (endoplasmic reticulum)
2.19	72661	<i>Serp2</i>	stress-associated endoplasmic reticulum protein family member 2
2.13	66753	<i>Erlec1</i>	endoplasmic reticulum lectin 1
2.03	12282	<i>Hyou1</i>	hypoxia up-regulated 1
1.99	59048	<i>C1Galt1c1</i>	Core 1 Synthase, Glycoprotein-N-Acetylgalactosamine 3-Beta-Galactosyltransferase 1 (C1GALT1)-specific chaperone 1
1.94	67838	<i>Dnajb11</i>	DnaJ (Hsp40) homolog, subfamily B, member 11
1.85	19711	<i>Resp18</i>	regulated endocrine-specific protein 18
1.77	14827	<i>Pdia3</i>	protein disulfide isomerase family A, member 3
1.67	27362	<i>Dnajb9</i>	DnaJ (Hsp40) homolog, subfamily B, member 9
1.64	81500	<i>Sil1</i>	SIL1 nucleotide exchange factor
1.62	19035	<i>PpiB</i>	peptidylprolyl isomerase B (cyclophilin B)
1.61	66940	<i>Shisa5</i>	shisa family member 5
1.61	216440	<i>Os9</i>	osteosarcoma amplified 9, endoplasmic reticulum lectin
1.59	20832	<i>Ssr4</i>	signal sequence receptor, delta
1.58	20316	<i>Sdf2</i>	stromal cell-derived factor 2
1.54	219134	<i>Shisa2</i>	shisa family member 2
1.53	26427	<i>Creb3l1</i>	cAMP responsive element binding protein 3-like 1
1.52	108687	<i>Edem2</i>	ER degradation enhancer, mannosidase alpha-like 2
1.50	378702	<i>Serf2</i>	small EDRK-rich factor 2
1.50	64209	<i>Herpud1</i>	homocysteine-inducible, endoplasmic reticulum stress-inducible, ubiquitin-like domain member 1
-1.61	14228	<i>Fkbp4</i>	FK506 binding protein 4
-1.68	319909	<i>Ism1</i>	isthmin 1, angiogenesis inhibitor
-1.87	12745	<i>Ctgn</i>	calmegin
-1.93	108960	<i>Irak2</i>	interleukin-1 receptor-associated kinase 2
-2.09	18111	<i>Nnat</i>	neuronatin
-2.23	26557	<i>Homer2</i>	homer scaffolding protein 2
-2.25	66256	<i>Ssr2</i>	signal sequence receptor, beta
-3.61	229722	<i>Kiaa1324</i>	KIAA1324

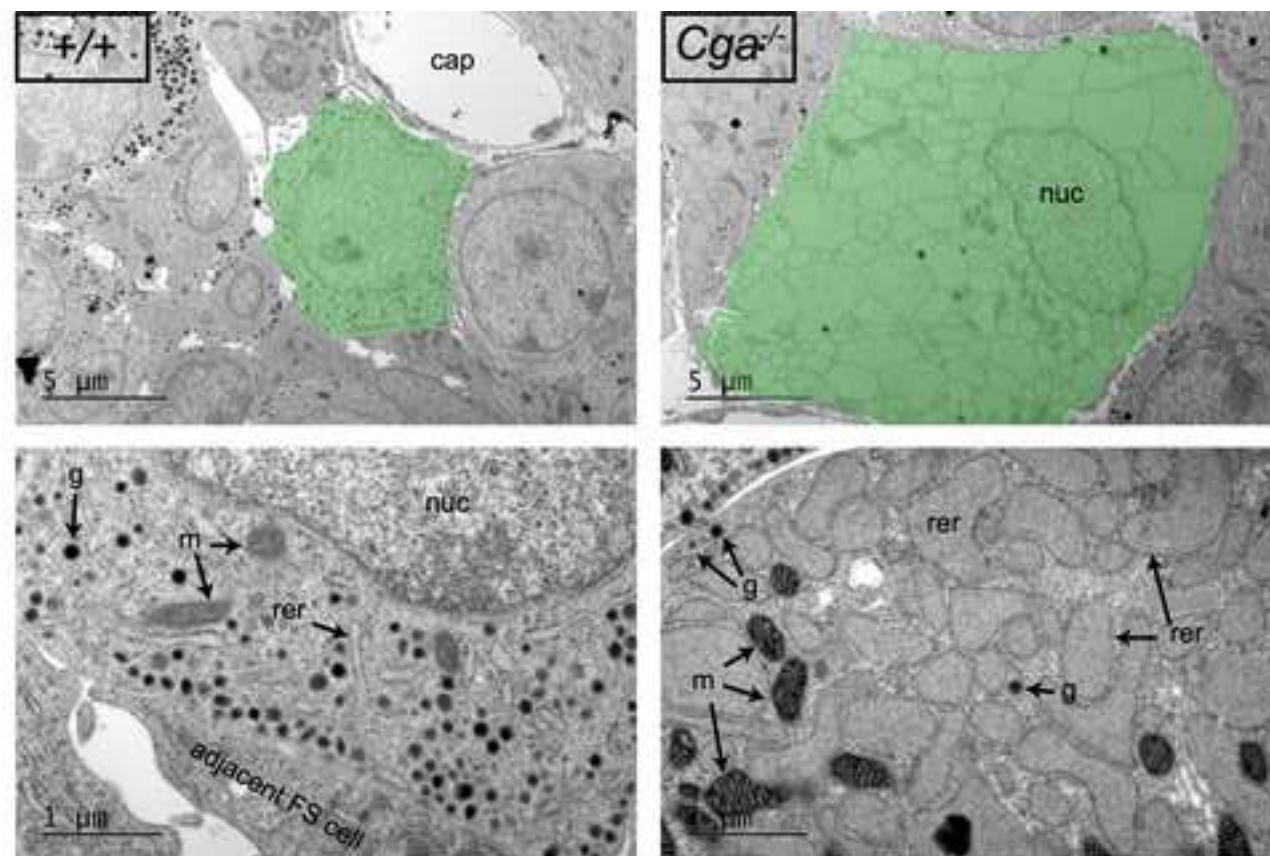
B

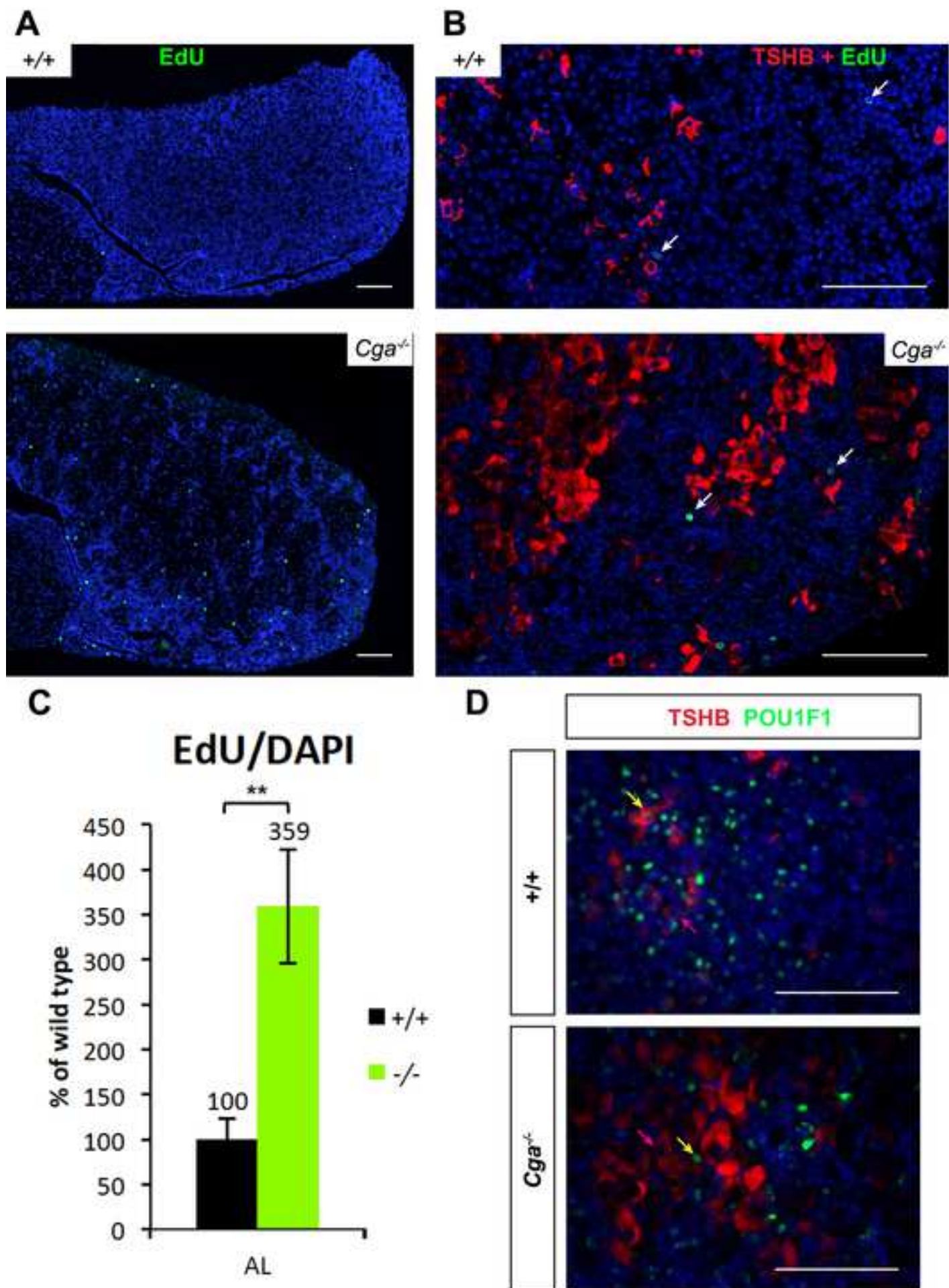
qPCR fold change	Entrez Gene ID	Symbol	Gene Name
46.91	56312	<i>Nupr1</i>	nuclear protein, transcriptional regulator, 1
4.05	331532	<i>Tceal5</i>	transcription elongation factor A (SII)-like 5
3.67	26427	<i>Creb3l1</i>	cAMP responsive element binding protein 3-like 1
3.60	13555	<i>E2f1</i>	E2F transcription factor 1
3.12	104156	<i>Etv5</i>	ets variant 5
2.75	14461	<i>Gata2</i>	GATA binding protein 2
2.59	16392	<i>Isl1</i>	ISL LIM homeobox 1
2.56	241494	<i>Znf385b</i>	zinc finger protein 385B
2.23	13198	<i>Ddit3</i>	DNA-damage-inducible transcript 3
1.67	20289	<i>Scx</i>	scleraxis basic helix-loop-helix transcription factor
1.55	72693	<i>Zcchc12</i>	zinc finger, CCHC domain containing 12
1.44	270118	<i>Maml2</i>	mastermind like 2
1.41	14199	<i>Fhl1</i>	four and a half LIM domains 1
1.17	406217	<i>Bex4</i>	brain expressed, X-linked 4
-1.66	231986	<i>Jazf1</i>	JAZF zinc finger 1
-2.00	16871	<i>Lhx3</i>	LIM homeobox 3
-2.08	17122	<i>Mxd4</i>	MAX dimerization protein 4
-2.33	192231	<i>Hexim1</i>	hexamethylene bis-acetamide inducible 1
-2.38	67087	<i>Cttnbp1</i>	catenin, beta interacting protein 1
-2.38	20747	<i>Spop</i>	speckle-type POZ protein
-2.56	15901	<i>Id1</i>	inhibitor of DNA binding 1
-2.56	18736	<i>Pou1f1</i>	POU class 1 homeobox 1
-2.63	11835	<i>Ar</i>	androgen receptor
-2.78	56458	<i>Foxo1</i>	forkhead box O1
-2.86	68705	<i>Gtf2f2</i>	general transcription factor IIF, polypeptide 2
-2.94	17341	<i>Bhlha15</i>	basic helix-loop-helix family, member a15
-2.94	60599	<i>Tp53inp1</i>	tumor protein p53 inducible nuclear protein 1
-3.13	20850	<i>Stat5a</i>	signal transducer and activator of transcription 5A
-3.23	13654	<i>Egr2</i>	early growth response 2
-3.45	68728	<i>Tp53inp2</i>	tumor protein p53 inducible nuclear protein 2
-3.70	16601	<i>Klf9</i>	Kruppel-like factor 9
-6.67	15460	<i>Hr</i>	hair growth associated
-12.50	66255	<i>Hsbp1l1</i>	heat shock factor binding protein 1-like 1

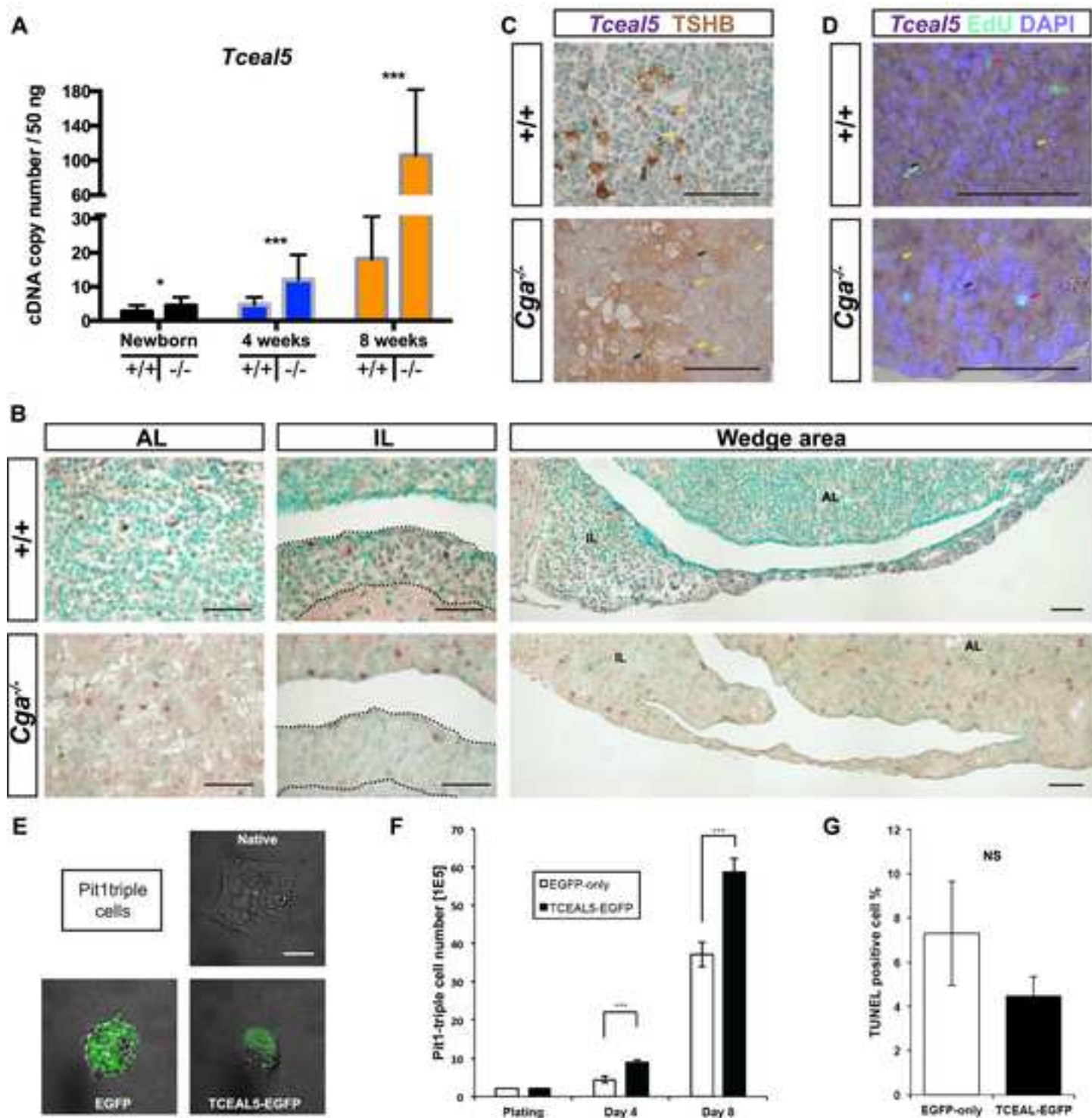
A



B







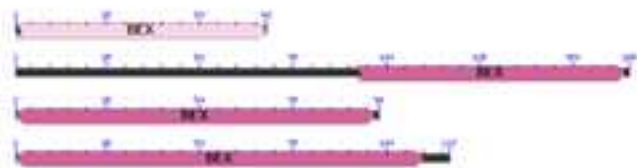
A

BEX domain

TCEAL1

TCEAL7

TCEAL8



BEX domain

TCEAL3

TCEAL5

TCEAL6

**B**

Mouse

Human

Dog

Chimpanzee

Horse

1 MEKLYKENEGKPEENKGRADEGST-----EGGK--ADEKSDAEGKPARCGKLEVEGGGEQAQKGEKPEKQKKSOGEGKRG-ESKPDQAKSASEARAAEKRPEDYVPRKAKRK 112
 1 MEKLYKENEGKPEENKLESGKPEDEGSTEDGKSDDEEKPDMEGKTECEGKREDEGERGDEGQLEDEGNQEKQKKSOGEGKPOS-EGKPDQAKSASEARAAEKRPEDYVPRKAKRK 119
 1 MEKLYKENEGKPEENKLESGKPEDEGSTEDGKSDDEEKPDMEGKTECEGKREDEGERGDEGQLEDEGNQEKQKKSOGEGKPOS-EGKPDQAKSASEARAAEKRPEDYVPRKAKRK 119
 1 MEKLYKENEGKPEENKLESGKPEDEGSTEDGKSDDEEKPDMEGKTECEGKREDEGERGDEGQLEDEGNQEKQKKSOGEGKPOS-EGKPDQAKSASEARAAEKRPEDYVPRKAKRK 119
 1 MEKLYKENEGKPEENKLESGKPEDEGSTEDGKSDDEEKPDMEGKTECEGKREDEGERGDEGQLEDEGNQEKQKKSOGEGKPOS-EGKPDQAKSASEARAAEKRPEDYVPRKAKRK 120

BEX

Mouse

Human

Dog

Chimpanzee

Horse

113 TDRGTDDSPKNSQEDLQRRHVSSEEMRECADHTRAQEELRKQKMGGFHVPDADQALVPRGORGVRGVRGGGRGQKDLQDAPFV 200
 120 TDRGTDDSPKNSQEDLQRRHVSSEEMRECADHTRAQEELRKQKMGGFHVPDADQALVPRGORGVRGVRGGGRGQKDLQDAPFV 206
 120 TDRGTDDSPKNSQEDLQRRHVSSEEMRECADHTRAQEELRKQKMGGFHVPDADQALVPRGORGVRGVRGGGRGQKDLQDAPFV 206
 120 TDRGTDDSPKNSQEDLQRRHVSSEEMRECADHTRAQEELRKQKMGGFHVPDADQALVPRGORGVRGVRGGGRGQKDLQDAPFV 206
 121 TDRGTDDSPKNSQEDLQRRHVSSEEMRECADHTRAQEELRKQKMGGFHVPDADQALVPRGORGVRGVRGGGRGQKDLQDAPFV 207

C

Mm TCEAL5

Mm TCEAL7

Hs TCEAL7

Mm BEX3





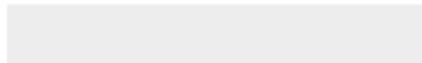




Click here to access/download
Supplemental Material
Supplemental Table 3.tif



Click here to access/download
Supplemental Material
Supplemental Video 1.mov



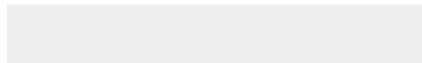


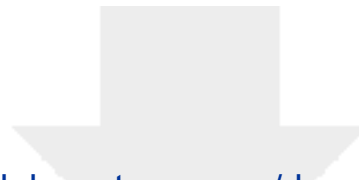
Click here to access/download
Supplemental Material
Supplemental Video 2.mov





Click here to access/download
Supplemental Material
Supplemental Video 3.mov

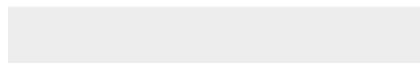




[Click here to access/download](#)

Supplemental Material

Supplemental Materials and Methods.pdf



Antibody Table

Peptide/protein target	Antigen sequence (if known)	Name of Antibody	Manufacturer, catalog #, and/or name of individual providing the antibody	Species raised in; monoclonal or polyclonal	Dilution used
Thyroid stimulating hormone	Beta subunit	anti-r TSH-beta	AF Parlow, Hormone Distribution Program, AFP967793	Guinea pig, polyclonal	1:20,000
Guinea pig IgG		Biotinylated anti-guinea pig IgG (H+L)	Jackson Immuno Research, #706-065-148	Donkey, polyclonal	1:200
Thyroid stimulating hormone	Beta subunit	anti-m TSH-beta	AF Parlow, Hormone Distribution Program	Rabbit, polyclonal	1:5,000
Rabbit IgG		15nm gold-conjugated goat anti-rabbit (H+L)	British Biocell, EM.GAR15	Goat, polyclonal	1:60